MASSACHUSETTS INSTITUTE OF TECHNOLOGY

LINCOLN LABORATORY

MILLSTONE HILL THOMSON SCATTER RESULTS FOR 1966

J. V. EVANS

Group 21

TECHNICAL REPORT 481

19 JANUARY 1971

LEXINGTON MASSACHUSETTS

Air Force (1) 16 June 1971 - 410

The work reported in this document was performed at Lincoln Laboratory, a center for research operated by Massachusetts Institute of Technology. The work is sponsored by the Office of the Chief of Research and Development, Department of the Army; it is supported by the Advanced Ballistic Missile Defense Agency under Air Force Contract F19628-70-C-0230.

ABSTRACT

This report presents F-region electron densities and electron temperatures observed during the year 1966 at the Millstone Hill Radar Observatory (42.6°N, 71.5°W) by the UHF Thomson (incoherent) scatter radar. The measurements were usually made for periods of 24 hours twice per month, and covered the altitude range 150 to 750 km approximately. The time required to collect all the measurements spanning this height interval was 30 minutes, i.e., half that of previous years. The results exhibit a greater amount of random time variation than seen heretofore, partly as a result of the better time resolution achieved and partly because each day has been analyzed individually, i.e., we have discontinued the practice of computing only the monthly mean behavior. We believe, however, that the largest part of the random variation is real and results from fluctuations in the solar EUV flux, which increase in magnitude as the sunspot number rises. Also, we expect a growing incidence of fluctuations produced by large-scale traveling ionospheric disturbances as we approach sunspot maximum. Despite this variability, the characteristics "winter" and "summer" type behavior reported for Millstone in previous years is clearly recognizable. On four days in which pronounced effects due to geomagnetic storms are evident, the layer rose to great heights in the late afternoon and achieved an abnormally high density (and lower-than-normal temperature). The reverse behavior was encountered the next morning. This sequence is similar to that first seen in June 1965, and its interpretation in terms of current ideas is summarized.

Accepted for the Air Force
Joseph R. Waterman, Lt. Col., USAF
Chief, Lincoln Laboratory Project Office

CONTENTS

	Abstract	iii
I.	INTRODUCTION	1
II.	EQUIPMENT, AND OBSERVING AND DATA-PROCESSING PROCEDURES	3
	A. Equipment	3
	B. Observing Procedures	3
	C. Data Reduction	3
III.	RESULTS FOR ELECTRON DENSITY	5
	A. Contour Plots	5
	B. Discussion	13
IV.	ELECTRON TEMPERATURE	14
	A. Contour Plots	14
	B. Average Temperature Profiles	21
V.	SEASONAL VARIATIONS	32
	A. Electron Temperature	32
	B. Protonospheric Heat Flux	35
VI.	SUMMARY	37
References		39

MILLSTONE HILL THOMSON SCATTER RESULTS FOR 1966

I. INTRODUCTION

Thomson (incoherent) scatter radar measurements of F-region electron densities and temperatures were made at Millstone Hill, Westford, Massachusetts (42.6°N, 71.5°W) approximately twice per month throughout 1966 for periods of 24 hours. This report summarizes the results obtained and discusses these in relation to the behavior observed in previous years. Earlier reports in this series[1-3] have presented the results of the synoptic studies carried out in 1963, 1964 and 1965. Results obtained in some of the months in these years have been presented in a number of journal articles which are listed in Table I.

TABLE I

PUBLICATIONS CONCERNING THE MILLSTONE HILL UHF (68-cm Wavelength) THOMSON SCATTER RESULTS

Year	Months Covered	Publication
1963	February 1963 to January 1964	Ref. 1
	March, July, August, September	Ref. 4
	April, July, November	Ref. 5
1964	January through December	Ref. 2
	April, July, November	Ref. 6
1965	January through December	Ref. 3
	June, August, September,	Refs. 7, 8
	June	Ref. 9
	January, April, July	Ref. 10

Section II summarizes the equipment, and observing and data-processing procedures employed during 1966. These differed little from those of the latter half of 1965, which are fully documented in Ref. 3. In Sec. III, we present the results obtained for electron density, and in Sec. IV those for electron temperature including average daytime and nighttime electron temperature profiles obtained for each 24-hour period. In Sec. V, these averages are employed to derive seasonal temperature variations and seasonal variations in the heat conducted into the F-region from the magnetosphere. A summary of the results is provided in Sec. VI.

TABLE II

INCOHERENT SCATTER OBSERVATIONS – 1966

Begin (EST)			End (EST)			Mean K_p	Comment
14 January	q	1100	15 January		1200	2–	
21 January	D	1200	22 January	D	1200	4_o	Very disturbed
25 February		1200	26 February	Q	1200	1_o	Quiet
11 March		1200	12 March		1200	2–	
16 March		1200	17 March		1200	1+	Quiet
1 April	D	1200	2 April	D	1200	3_o	Disturbed
28 April		1700	29 April		1500	1+	Quiet
12 May		1300	13 May		0800	2_o	Portion lost
28 June		1600	29 June		1600	2–	
11 July		0700	12 July	D	0900	3–	Disturbed
14 July	Q	1500	15 July		1500	1–	Quiet
17 August	Q	1100	18 August		1200	1+	Quiet
22 August	Q	1200	23 August	D	1300	3_o	Disturbed
12 September		1000	13 September		1000	1+	Quiet
26 September		1000	27 September		1000	4–	Disturbed
10 October	q	1600	11 October	Q	1400	0+	Quiet
20 October	q	1100	21 October	Q	1100	0	
7 November	q	1200	8 November		1200	2_o	
28 November	D	1600	29 November	D	1700	3_o	Disturbed
5 December	D	1200	6 December		1200	2+	
20 December		1200	20 December		1600	3_o	
21 December		0600	22 December		0700	2+	

II. EQUIPMENT, AND OBSERVING AND DATA-PROCESSING PROCEDURES

A. Equipment

The UHF radar equipment has been described previously. No major changes were made in 1966. The Millstone Hill C-4 ionosonde which had been inoperative during much of 1965 was brought into routine operation during 1966, thus obviating the need to depend on measurements of f_oF2 made elsewhere (Fort Belvoir, Virginia) to establish the absolute scale of the electron density profiles.

B. Observing Procedures

In 1965, the observing procedures were changed to reduce from 1 hour to 30 minutes the amount of time required to obtain a complete electron density and temperature profile. This was accomplished by recording the IF signals for later non-real-time processing. The recording and playback system, discussed extensively in Ref. 3, was employed throughout 1966.

In addition to this change, the spectrum analyzer was modified in June 1965 to permit both halves of the signal spectrum to be explored. Unfortunately, this was carried out in a way which, though not recognized at the time, caused some loss of information. As a result, the values for the ion temperature obtained are unreliable between about 300 and 500 km, and therefore are not included in this report. These changes and means of minimizing the unwanted effects they introduced in the results are discussed in Ref. 3 and will not be repeated here.

During 1966, we attempted to make observations twice per month for a period of 24 hours. Table II lists the dates and times on which measurements were carried out, together with the mean K_p index over the period of observation.

C. Data Reduction

Although the measurements obtained during 1965 yielded a time resolution of 30 minutes, we were obliged to construct plots of the temperature and density averaged over hourly intervals in order to reduce the scatter of the measurements. Further, because the measurements were made only once a month for 48 hours, results obtained on consecutive days were, as a rule, averaged to obtain the hourly mean profile. Thus, the 1965 results, like those obtained in previous years, were reduced to yield plots showing the mean hourly behavior for each calendar month. In reducing the results presented here, we attempted to preserve the 30-minute time resolution afforded by the observing procedure. Thus, for each 24-hour period, the measurements have been reduced to yield approximately 48 height profiles of electron density, and electron and ion temperatures. Furthermore, because of the increased solar activity encountered in 1966, the day-to-day similarity of the behavior was reduced; hence, each 24-hour measurement period has been treated separately. Table III contrasts this procedure with that for earlier measurements.

The electron density profiles were obtained from the radar measurements in the manner employed hitherto, namely, by combining measurements made with 0.1-, 0.5- and 1.0-msec pulses using a graphical overlay method. This combined smooth "power" profile was then corrected for the variation of the electron cross section with height resulting from the altitude variation in electron-to-ion temperature ratio T_e/T_i. Complete machine reduction of these data was made possible in 1968, following the construction of a new spectrum analyzer that is interfaced with the computer.[11]

TABLE III

OBSERVING PROGRAM AS A FUNCTION OF YEAR

Year	Length of Each Observing Period (hours)	No. of Observing Periods per Month	Time Taken to Measure One Profile (hours)	No. of Profiles Obtained per Month	Reduction Method Employed
1963	30	4	1.5	80	Mean hourly profiles constructed for each calendar month
1964	30	2	1.0	60	As above
1965	48	1	0.5	96	As above
1966	24	2	0.5	96	Each profile reduced separately

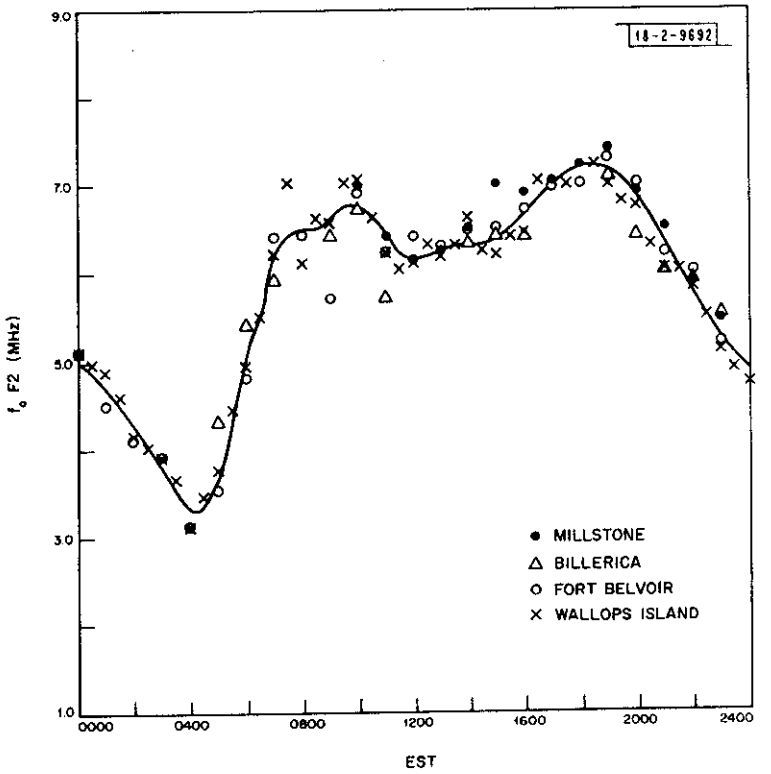

Fig. 1. Plot of f_oF2 obtained at four stations on 14 July 1966, and assumed local variation (solid line).

As in previous years, the absolute scale for the electron density profile measurements has been established by normalizing the density at the peak of the layer to match the value of N_{max} observed from ionosonde measurements. One change made during 1966 was to broaden the basis for the diurnal variation of f_oF2 by combining measurements made at the following stations

Billerica, Massachusetts	42°N, 71°W
Fort Monmouth, New Jersey	40°N, 74°W
Wallops Island, Virginia	37°N, 75°W

in addition to the values obtained from the C-4 ionosonde at Millstone. In order to combine the results, the values of f_oF2 reported by all four stations were plotted and a smooth curve drawn through as shown in the example of Fig. 1. In general, the variation seen at Millstone was followed except where this disagreed with all three of the other stations. The variation observed at Billerica (approximately 10 km from Millstone) should be expected to be extremely close to that observed locally, but in several instances was found to differ considerably from all three other stations -- suggesting errors of scaling.

III. RESULTS FOR ELECTRON DENSITY

A. Contour Plots

The combined density profiles were assigned absolute values in the manner outlined above. These density profiles were next given a scale of corresponding plasma frequency in 0.5-MHz intervals. A contour diagram showing the height at which a given plasma frequency is to be found as a function of local time was then constructed. Figure 2 provides an example of one of these diagrams, in which all the points have been connected by straight lines.

Subsequently, these contour diagrams were traced to yield smooth contours. Results for the periods listed in Table II are presented in Figs. 3(a) through (u). The smoothing operation is necessary to remove the influence on the diagrams of occasional bad profiles and structure with a 30-minute periodicity due to random errors of measurement. It is, however, a somewhat subjective process since there is no sure way of deciding what is true variation and what is not. As a rule, we have tended to de-emphasize marked fluctuations in the contours which are introduced by a single density profile. Despite this, the results [Figs. 3(a-u)] show considerably more structure than any that have been presented hitherto (Refs. 1, 2 or 3).

There are a number of reasons for the greater amount of structure in Figs. 3(a-u) than in earlier diagrams of this type. Previously, all plots were monthly means constructed by averaging all the data obtained in each of 24 hourly intervals during a given calendar month. These profiles were adjusted to have the same value of $h_{max}F2$ as their mean and then averaged to obtain a mean shape. Finally, they were normalized to have the mean value of $N_{max}F2$. Thus, day-to-day and hour-to-hour variations tended to be smoothed out. In addition, some time resolution was lost because a mean profile was constructed for each hour, irrespective of the time required to collect the results. Finally, the contours in Figs. 3(a-u) display more structure owing to a real increase in the variability of the ionosphere with increasing sunspot number.

The increase in sunspot activity gives rise to irregularities in the ionospheric behavior directly through fluctuations in the intensity of its ionizing radiations, and less directly through geomagnetic storm effects. As noted in the 1965 results, intense magnetic storms can give rise to large variations in the electron density.[7-9] The principal effect appears to be a lowering of the abundance of atomic oxygen relative to molecular nitrogen, with a consequent reduction in the peak density.[12-15] However, increases in density during the late afternoon have also been

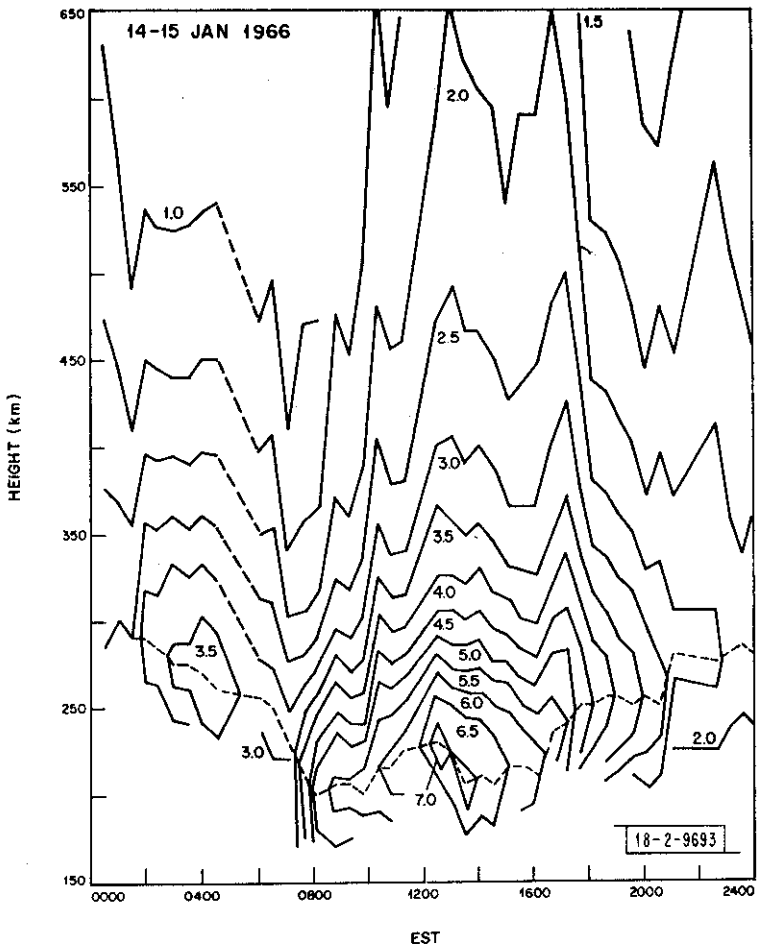

Fig. 2. Plasma frequency contour diagram constructed from electron density profiles obtained at 30-minute intervals for 24-hour period on 14-15 January 1966.

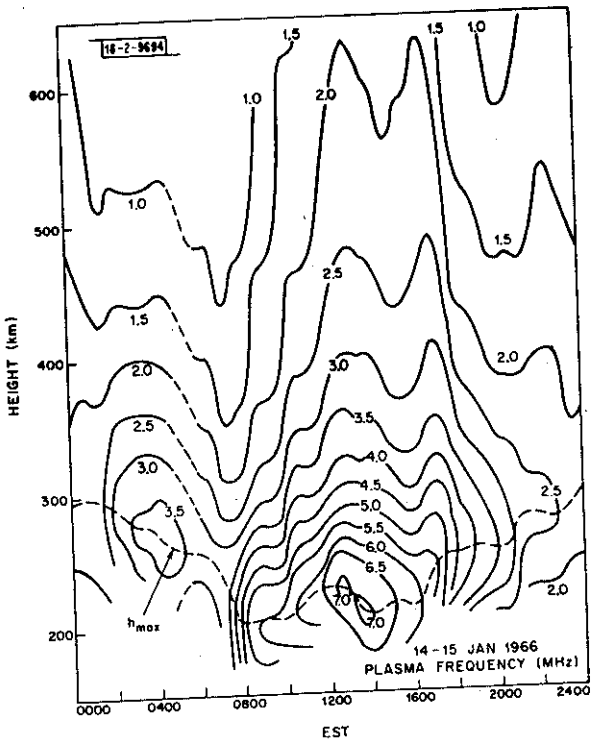

(a)

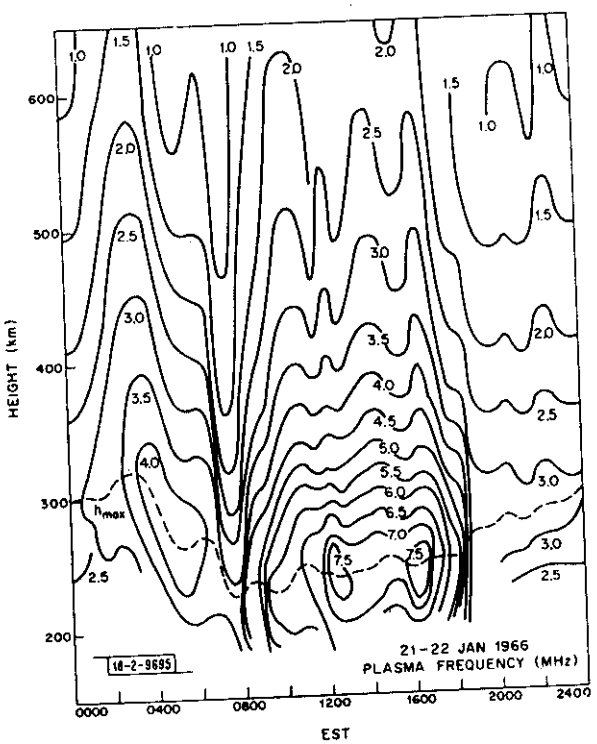

(b)

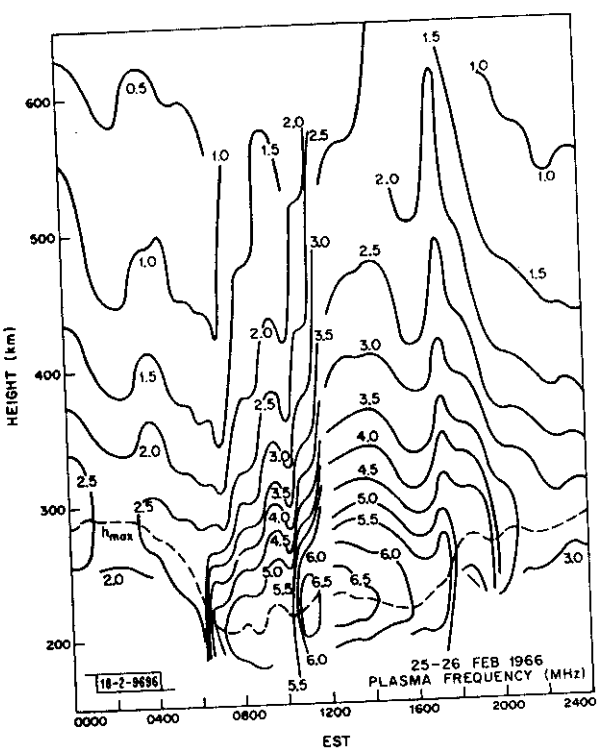

(c)

Fig. 3(a-u). Smoothed contour diagrams of plasma frequency vs height and time obtained for 24-hour periods in 1966.

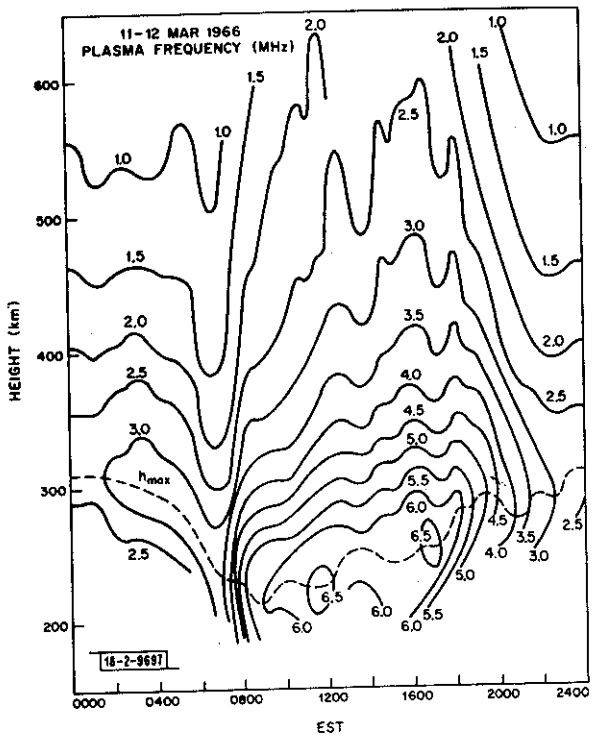

(d)

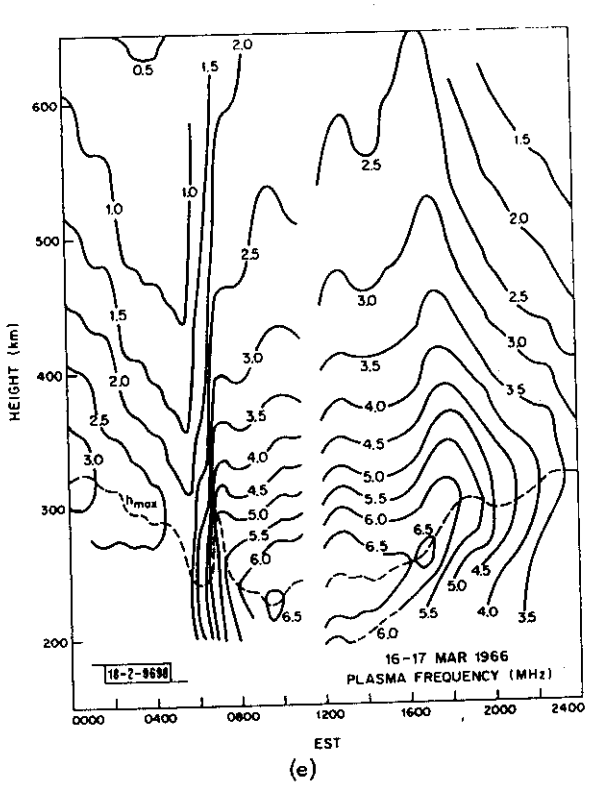

(e)

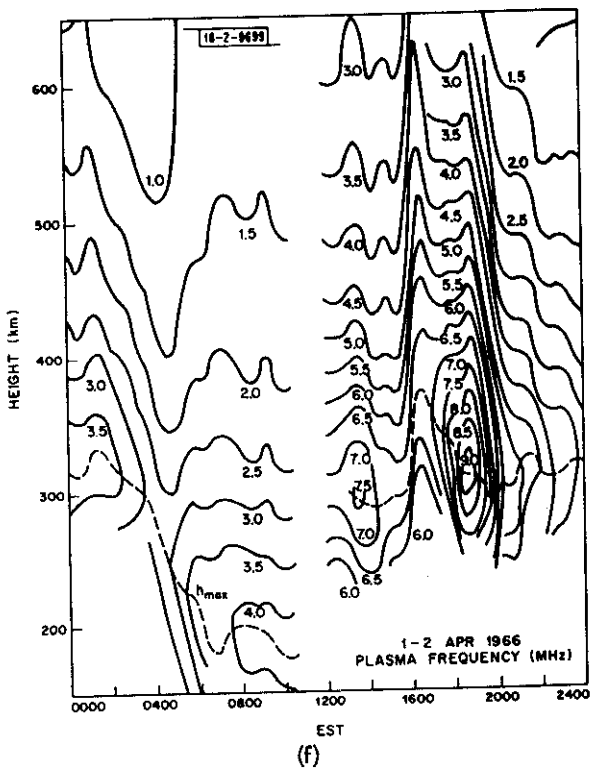

(f)

Fig. 3(a-u). Continued.

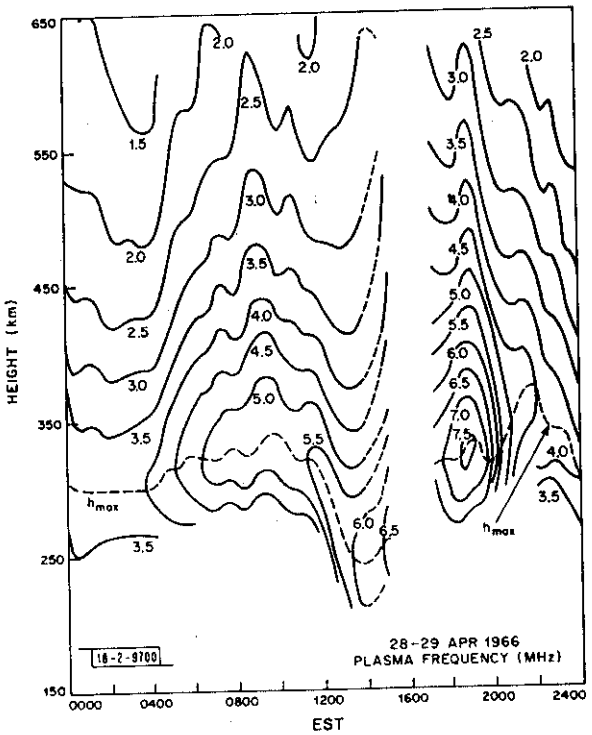

(g)

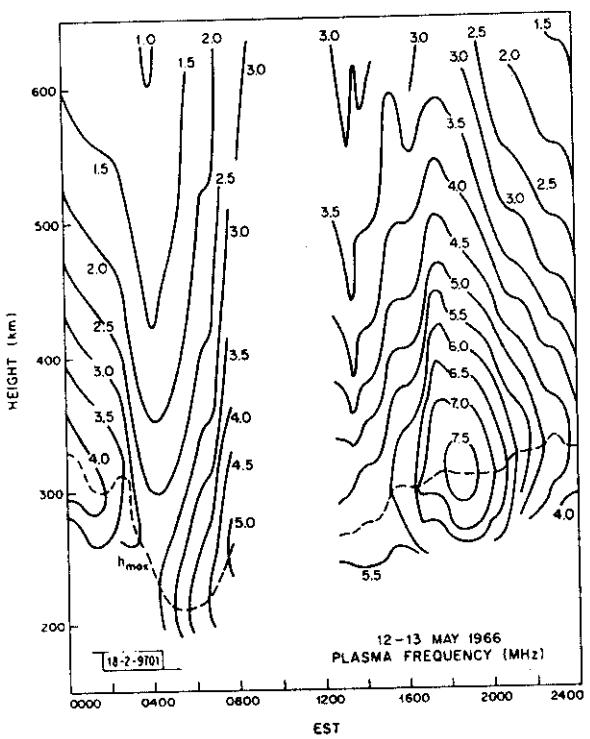

(h)

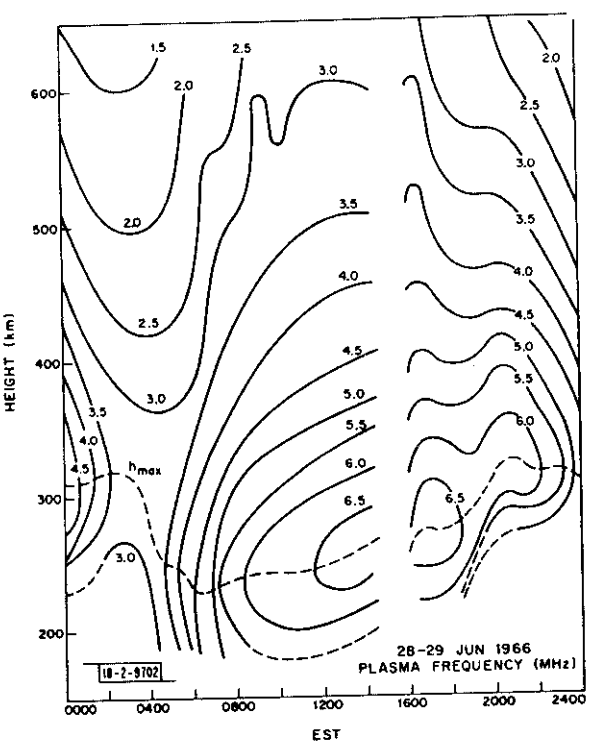

(i)

Fig. 3(a-u). Continued.

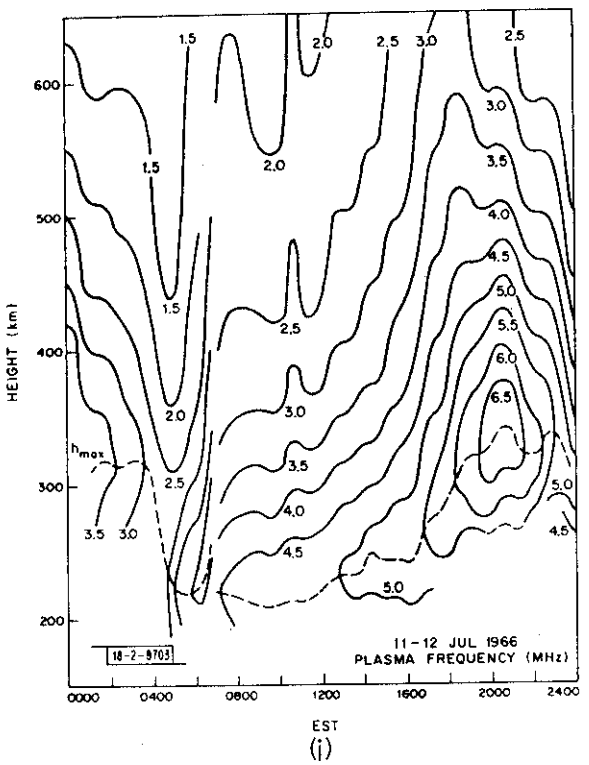

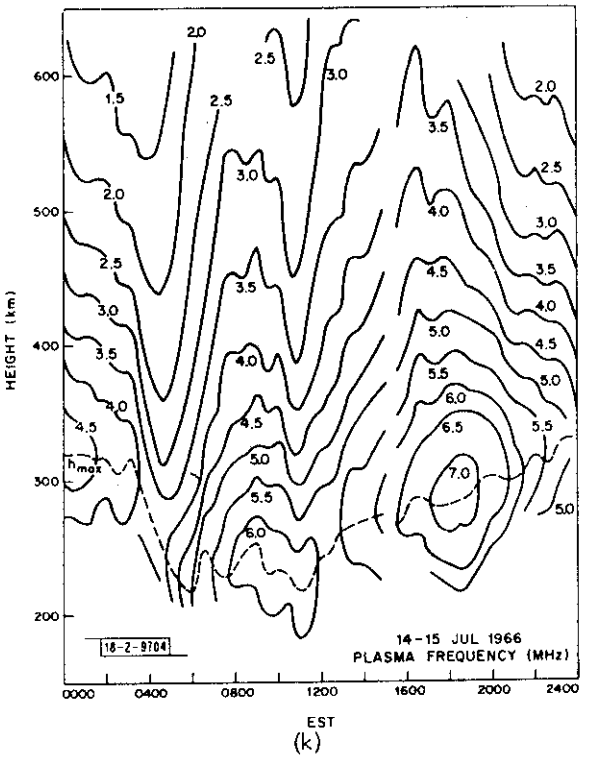

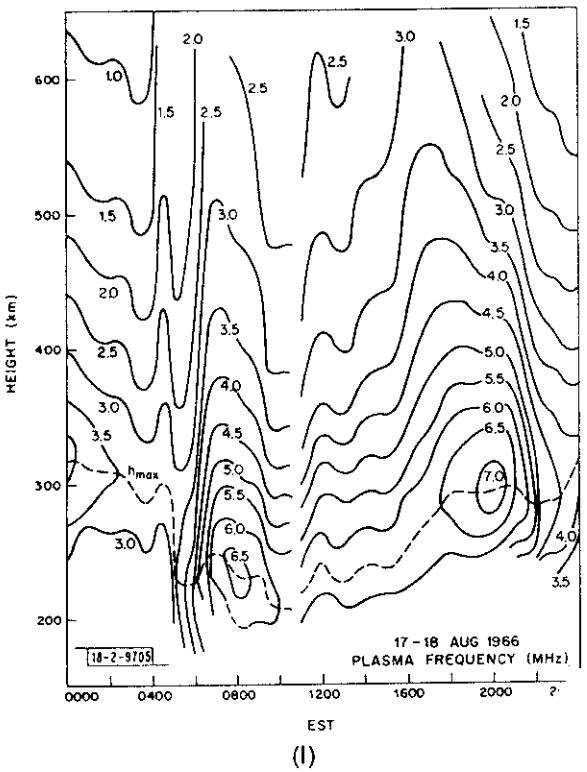

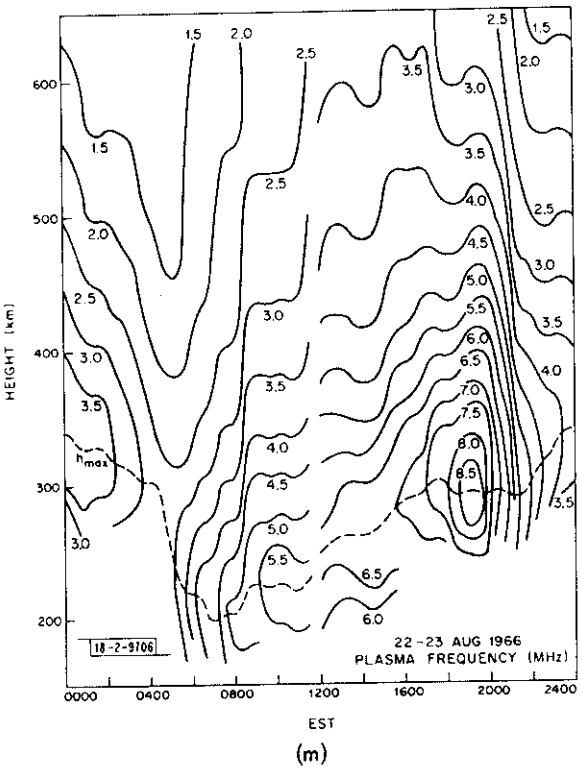

Fig. 3(a-u). Continued.

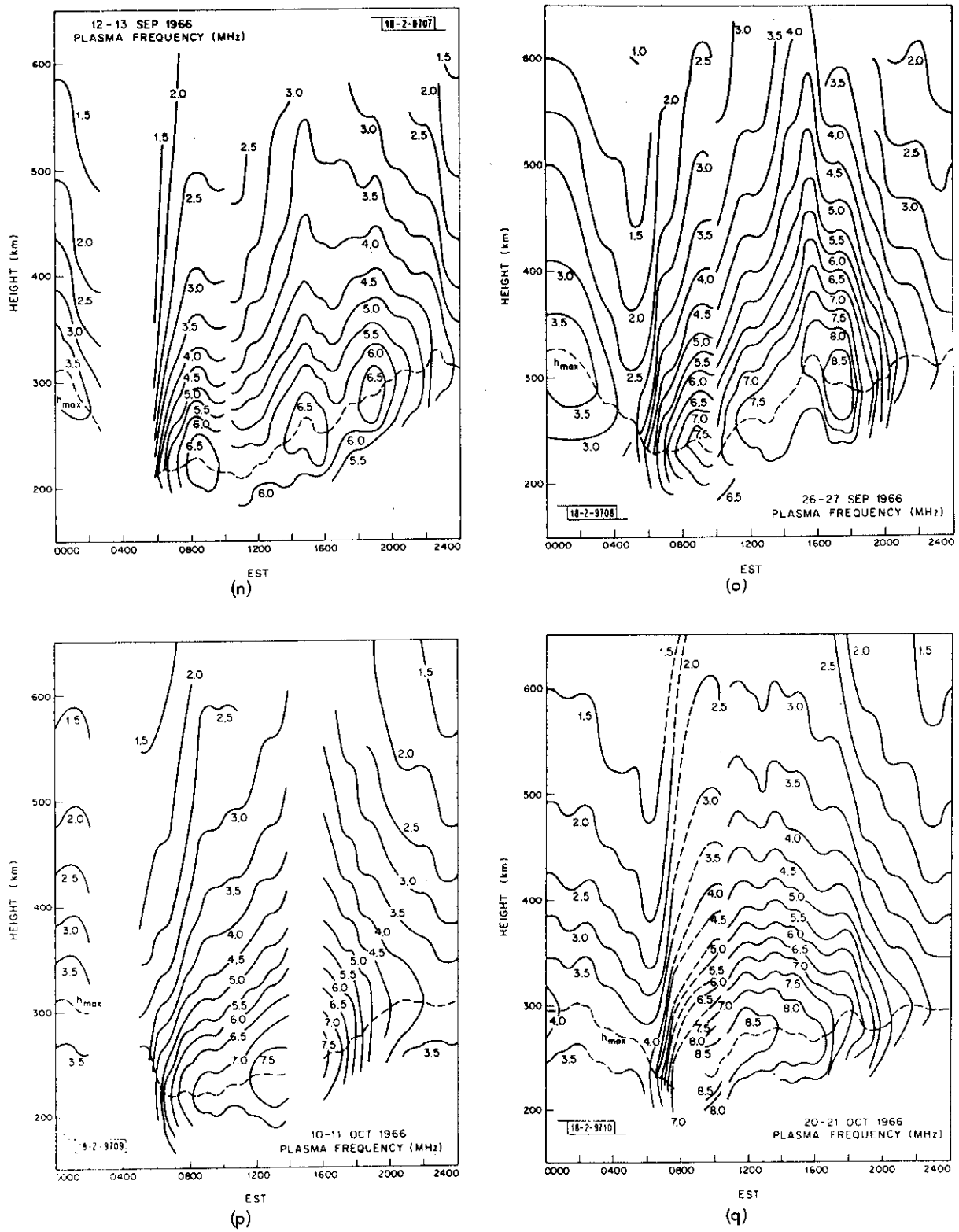

Fig. 3(a-u). Continued.

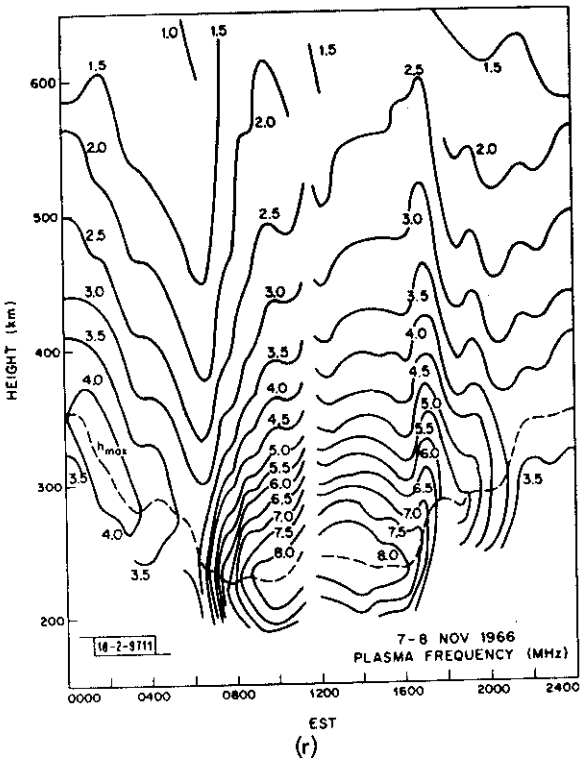

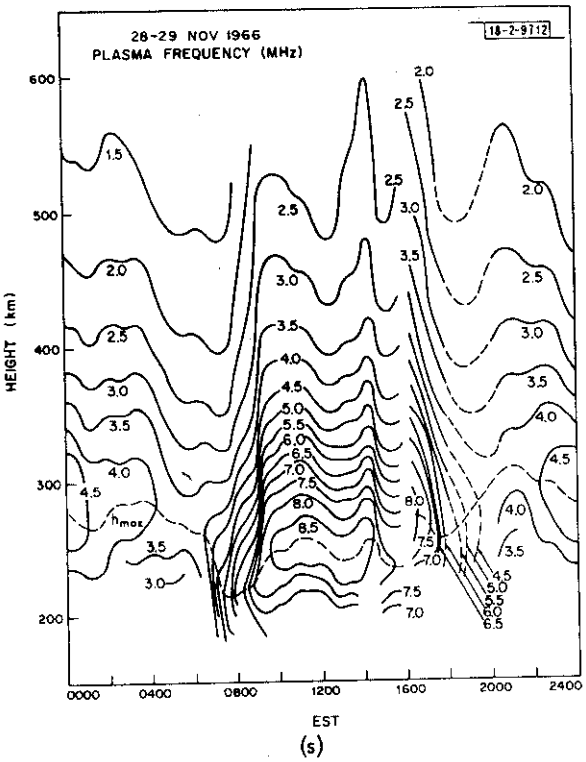

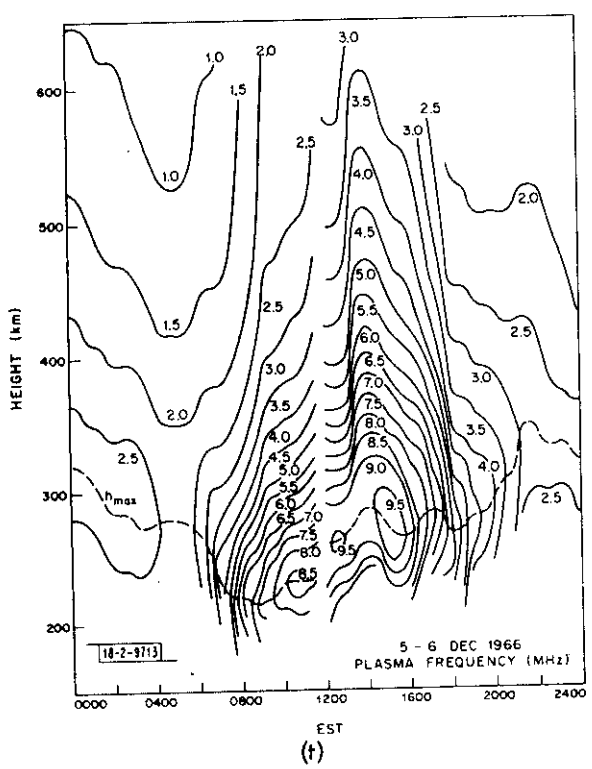

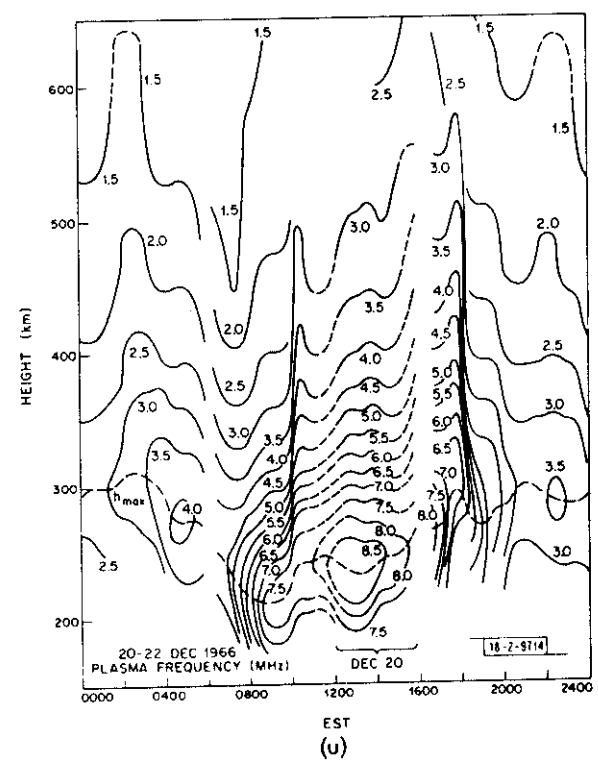

Fig. 3(a-u). Continued.

found which we have attributed to the influence of the electric field associated with the asymmetric part of the ring current.[9] Of the days listed in Table II, we would class only six as disturbed, i.e., with an average K_p value for the period of greater than 2+. Thus, we do not believe that all the variability found here can be attributed to storm effects; some may be caused by large-scale traveling ionospheric disturbances,[16,17] since these too occur with increasing frequency during years of high sunspot number. Traveling ionospheric disturbances are thought to be set up by the heating of the atmosphere produced by the auroral electrojet[18-20] and, as such, the occurrence of large disturbances is correlated with magnetic activity. Large-scale traveling ionospheric disturbances frequently have periods of the order of $\leq$30 minutes, and thus are not always properly resolved in our measurements.

B. Discussion

We have noted earlier[10] that the F-region electron density observed at Millstone has a characteristic "winter" and "summer" diurnal behavior with a rapid transition between the two in the equinox. This pattern can be seen in the contour diagrams of Figs. 3(a-u). The first three and the last six diagrams are fairly representative samples of the type of winter behavior we have discussed before. On these days, the F-layer critical frequency rose to a value of $\geq$7 MHz for a few hours centered on 1300 EST, and fell rapidly during the late afternoon. In most cases, a small predawn increase can be observed – a phenomenon described in Ref. 21 where it was attributed to ionization diffusing out of the protonosphere following conjugate sunset. Subsequently, we abandoned this explanation since the time of the increase (usually near 0400 EST) cannot be reconciled with the time the sun is lowest at the conjugate point.[6] It would seem that the source of the ionization must be the protonosphere, but that the timing of the increase is tied to neutral winds which at night serve to drive ionization up the field lines and thus raise $h_{max}F2$ and lower the loss rates.[22,23] It may be noted that the time of the increase can be as early as 0200 EST (7-8 November) or as late as 0430 EST (20-22 December). Similar variations have been found from observations of the total electron content of the ionosphere,[24] and may imply changes in the pattern of the neutral winds in the thermosphere brought about, for example, by heat deposited in the auroral zones.

The behavior observed on 11-12 March is somewhat unusual. While exhibiting a winter-type predawn enhancement, the main peak on this day is shifted into the late afternoon. This is the chief characteristic of the summer behavior[4] and is produced in part by the rapid redistribution of ionization above $h_{max}F2$ at sunset.[5] Virtually all the days between 11-12 March and 26-27 September exhibit this type of behavior. In 1965, we observed that the transition from winter- to summer-type behavior occurred in April.[3,10] In point of fact, measurements of the diurnal variation of f_oF2 show that the transition from one type of behavior to the other is not completed all at once. Near the time of transition, there are often days of one type followed by days of the other type interspersed at random. Thus, the timing of the transition as seen in our data depends on the actual behavior on the days selected for observation in equinox.

Typical summer-type behavior is exhibited in our data on 12-13 May, 11-12 and 14-15 July. On some days, e.g., 17-18 August and 26-27 September, there is a distinct forenoon peak. The presence of both morning and evening peaks has given rise to the so-called "bite-out" phenomenon that has long fascinated ionospheric workers.[25,26] Based upon recent evidence, it would seem that the bite-out is caused by the lowering of h_{max} during the daytime brought about by neutral winds,[22,23,27] together with a change in the composition of the neutral atmosphere in summer that increases the loss rates.[14,28-31]

Several days show two or more successive peaks in the electron density (e.g., 12-13 September and 5-6 December) together with fluctuations in $h_{max}F2$ that are suggestive of the presence of a large traveling ionospheric disturbance (TID). However, neither of the days mentioned was magnetically disturbed, so that one cannot say with certainty if indeed this is the correct explanation.

Of the six days listed in Table II as "disturbed," four days (viz., 21-22 January, 1-2 April, 22-23 August and 26-27 September) exhibit behavior that is very similar to the pattern observed during the major magnetic storm of June 1965 and discussed in Ref. 9. On those days, the evening increase was much more pronounced than normal, and was associated with a large increase in $h_{max}F2$. We believe that this phenomenon is caused by the presence of an electric field which serves to drive the layer via E × B drift upward into regions where the loss is reduced. We have suggested[9] that this field is conducted into the F-layer along lines of magnetic force from the magnetosphere where it is produced by charge separation of the electrons and protons associated with the asymmetric part of the ring current. Since the injection of the plasma into the ring current occurs principally in the evening sector, this explanation readily accounts for the phenomenon being seen only in the late afternoon, and is associated with positive increases in the total field observed locally. Mendillo, et al.,[32] who have studied this same phenomenon via measurements of total electron content, confirm these findings but attempt to explain them in terms of precipitation of ionization from the protonosphere. In the absence of measurements of the vertical transport of ionization during these increases, it is difficult to reject this explanation, although it fails to account for the increases always occurring before sunset, i.e., when production is still taking place.

Following these pronounced evening increases, the layer was formed at a very low altitude the next morning and exhibited a low peak density. Along with others,[12-15] we have attributed this to an increase in the abundance of N_2 relative to O in the F-region.[9] In essence, the F2 peak is reduced and one is left with an F1-layer. The change in the neutral atmosphere is believed to result from the increased temperature (which serves to increase N_2 and O in the F-region) together with the establishment of a thermospheric wind pattern that differs from the normal one, and appears to transport O from high and temperate latitudes toward the equator. Possibly the heating of the atmosphere in the auroral zone is responsible for this change.

It may be noted that the most disturbed day on which measurements were made during 1966 was 21-22 January (Table II). However, the behavior on this day does not differ very greatly from that observed on 14-15 January. It seems, in fact, that magnetic storms occurring in summer give rise to more pronounced effects than those in winter. This would suggest that the heating produced in the auroral zones by magnetic storms does not completely disrupt the normal thermospheric wind system, but serves to modify it. In the summer hemisphere, the effect is to reinforce the tendency for O to be depleted relative to N_2, whereas in the winter hemisphere the two effects (the seasonal increase in O and the storm-time depletion) appear offset to one another.

IV. ELECTRON TEMPERATURE

A. Contour Plots

Contour plots of electron temperature vs altitude and time have been constructed essentially in the same manner as those for electron density, and are presented in Figs. 4(a) through (u). Like the electron density contours, these too display more structure than has been noted hitherto, and probably the same reasons apply (see Sec. III).

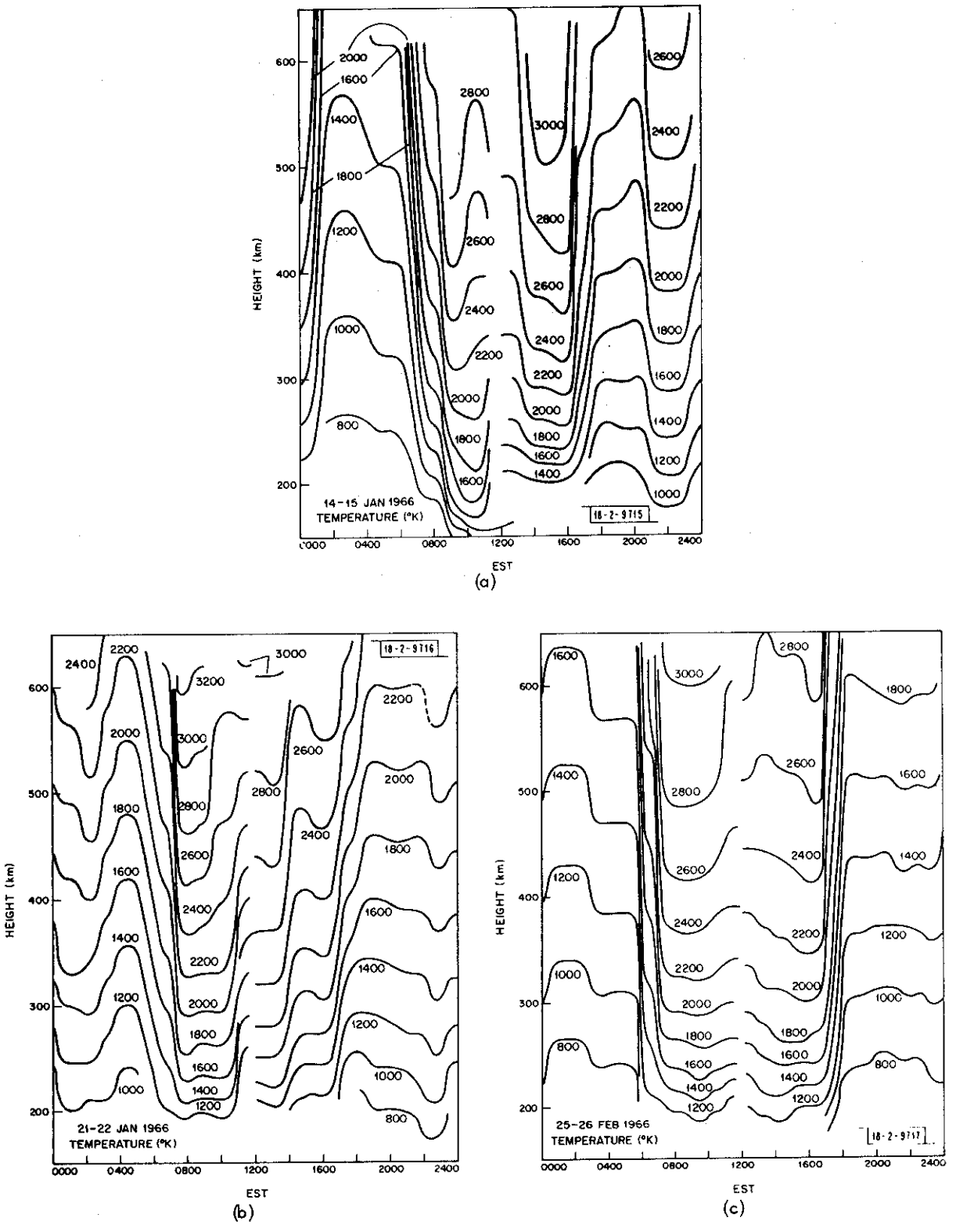

Fig. 4(a-u). Smoothed contour diagrams of electron temperature vs height and time obtained for 24-hour periods in 1966.

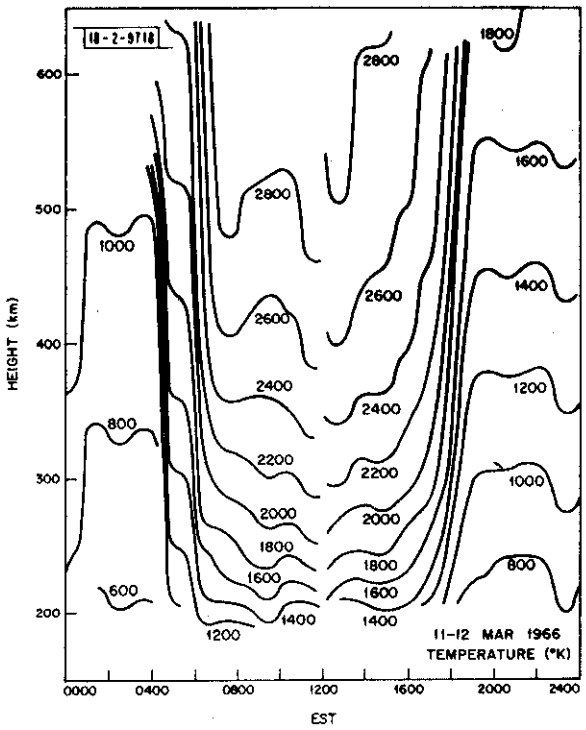

(d)

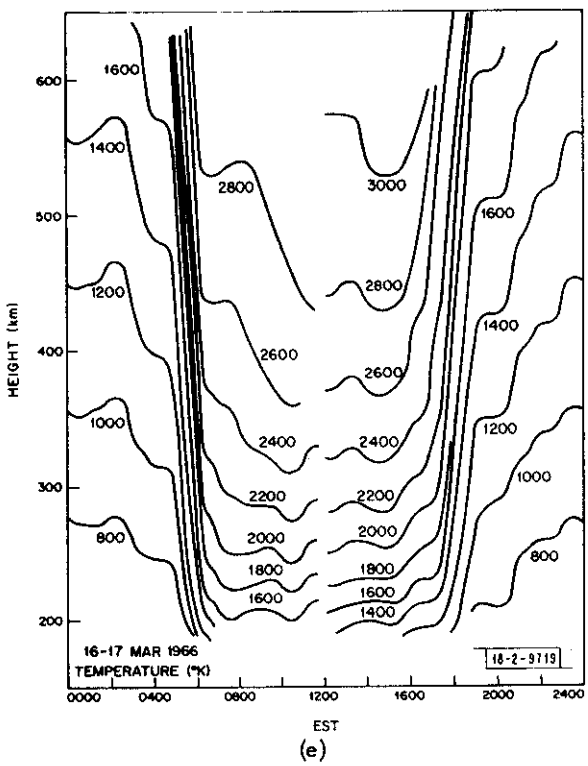

(e)

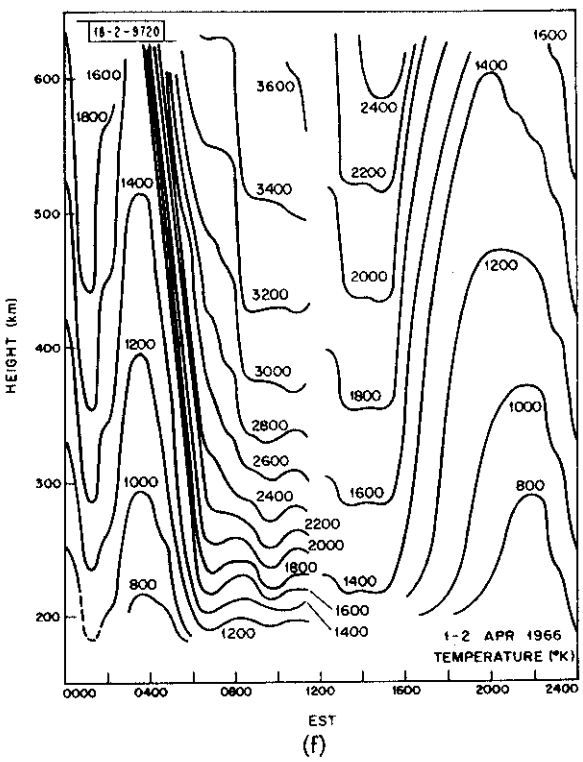

(f)

Fig. 4(a-u). Continued.

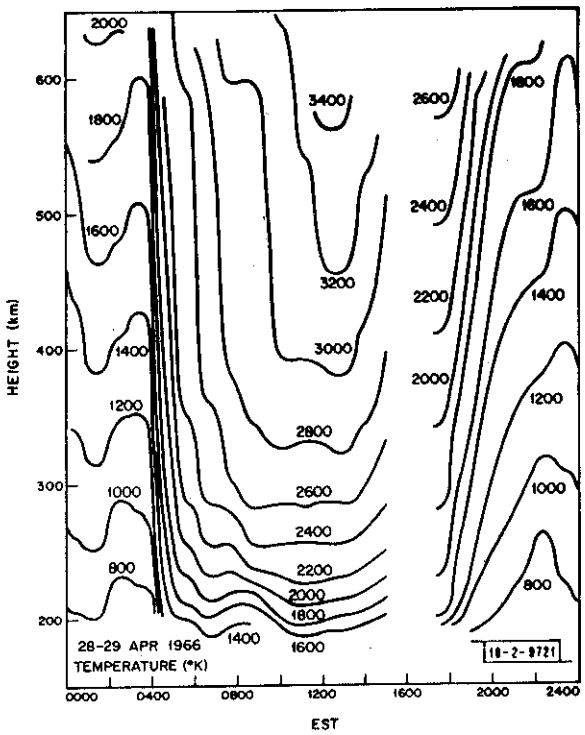

(g)

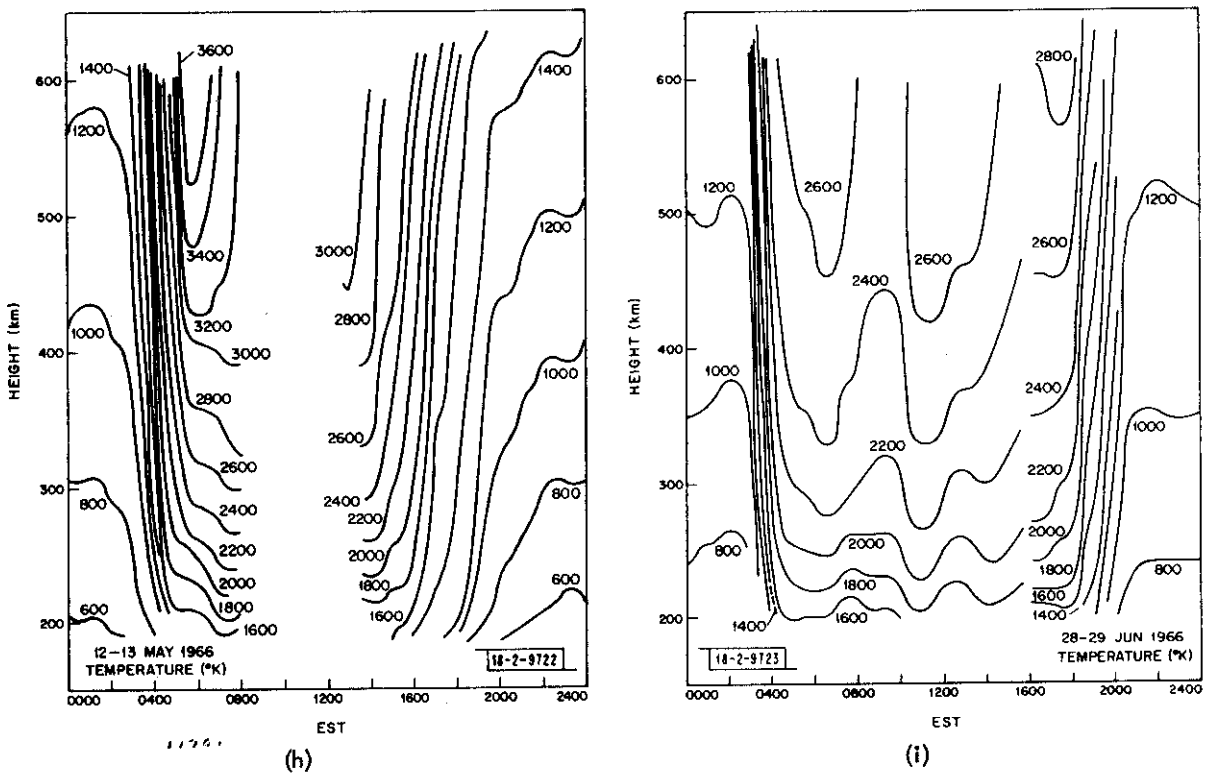

(h) (i)

Fig. 4(a-u). Continued.

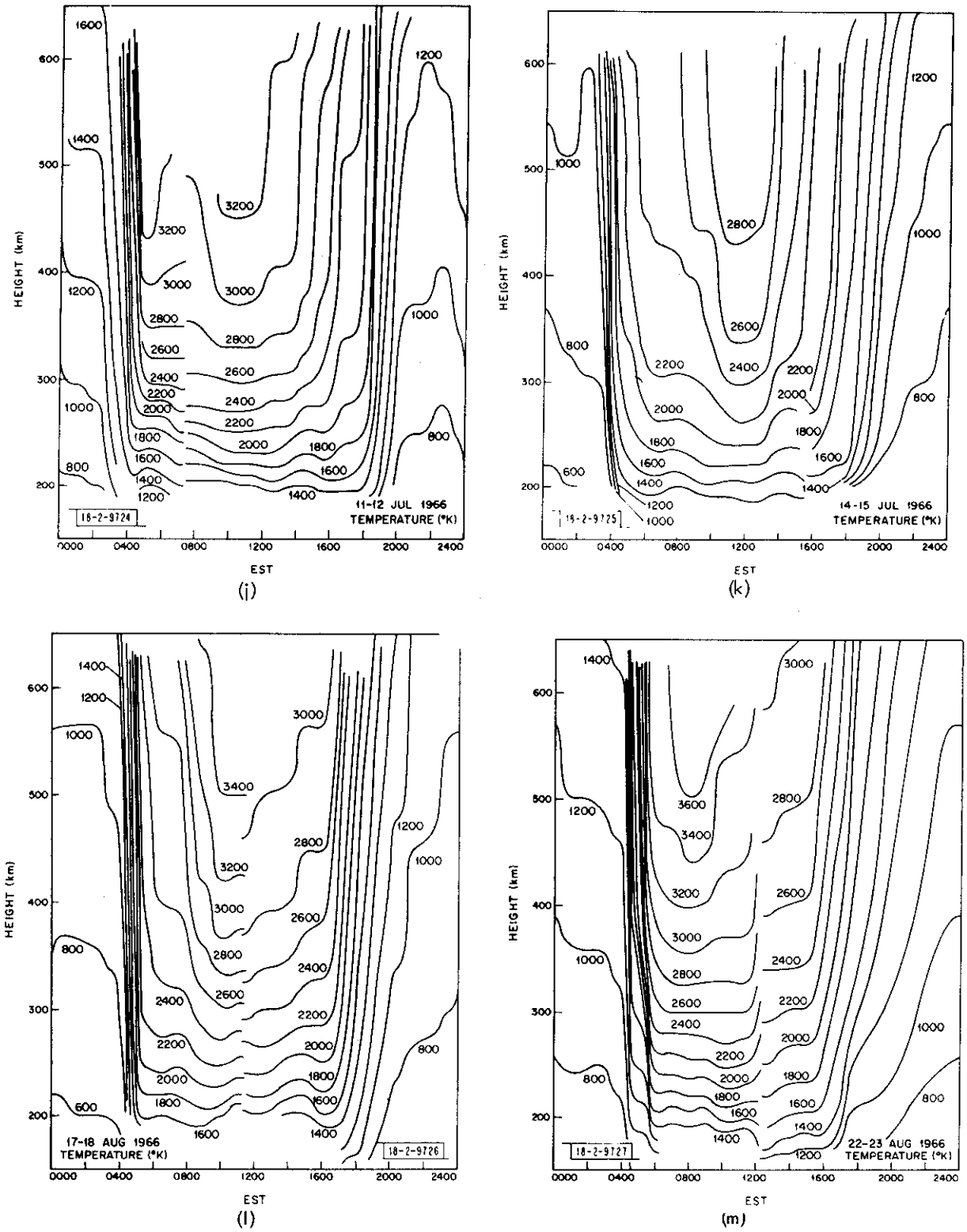

Fig. 4(a-u). Continued.

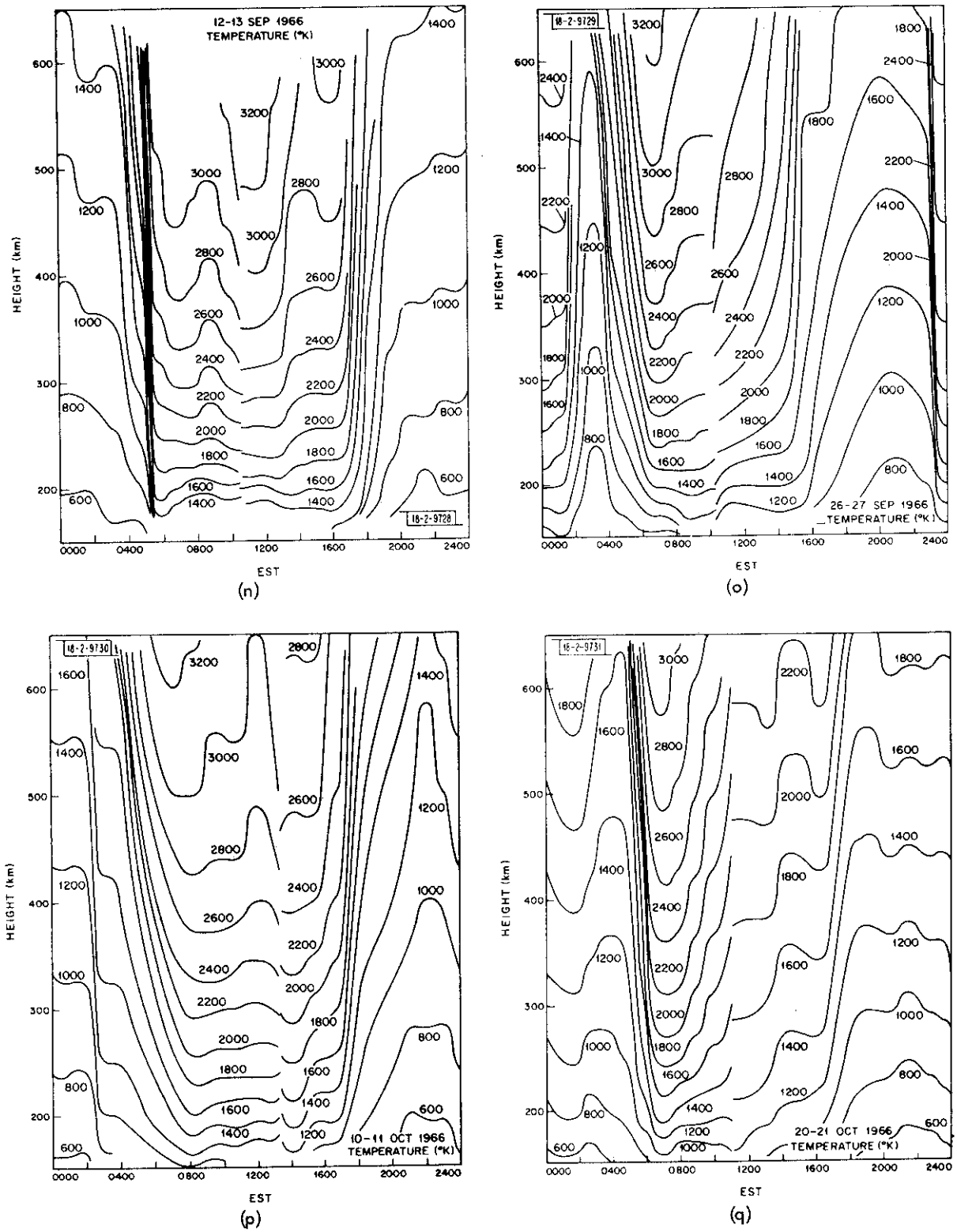

Fig. 4(a-u). Continued.

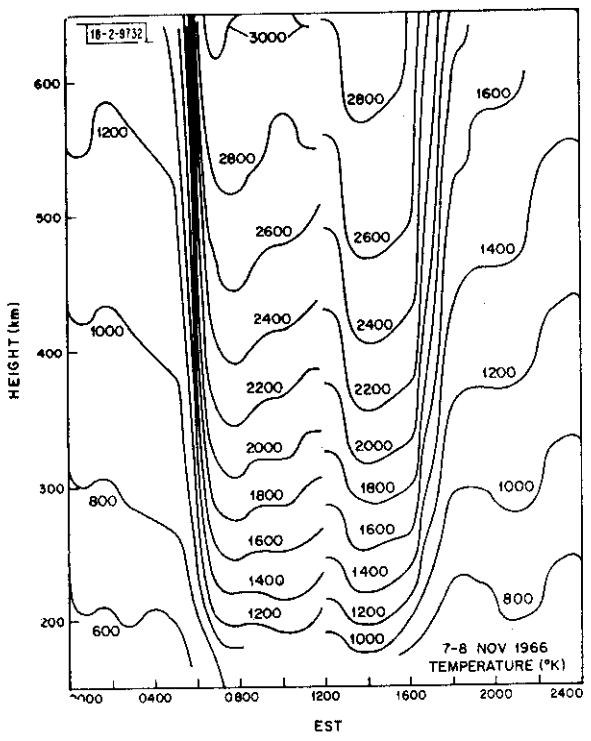

(r)

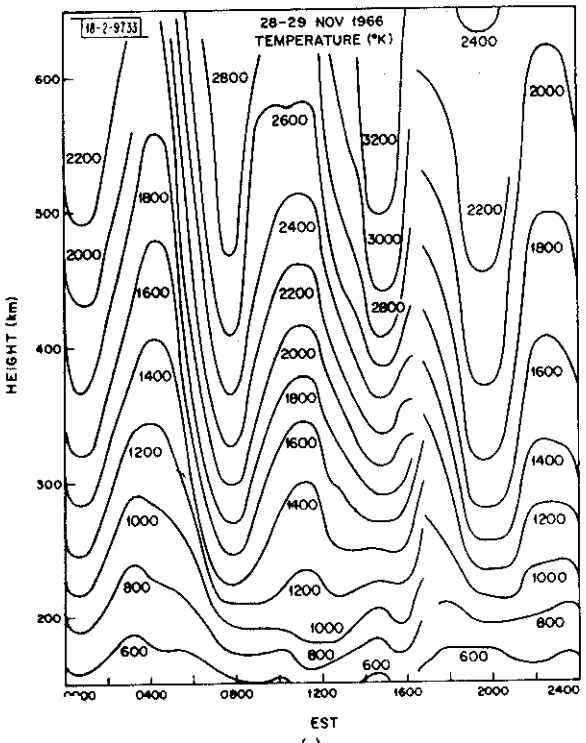

(s)

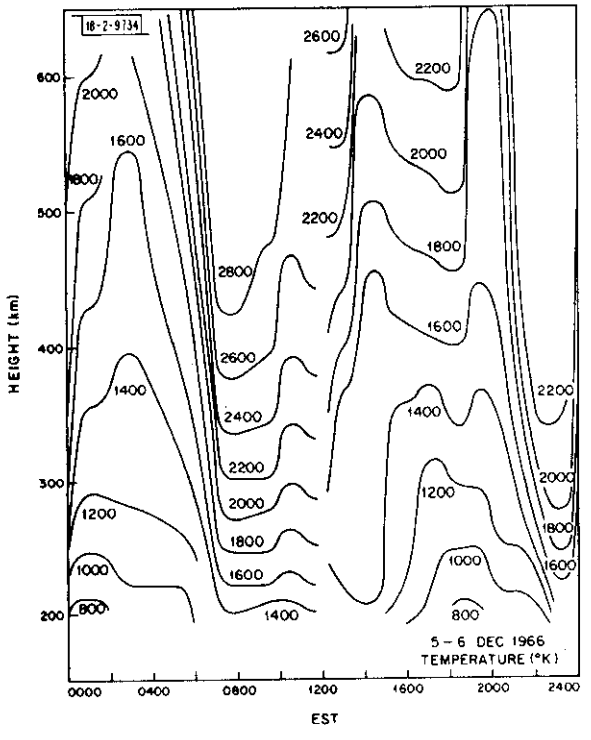

(t)

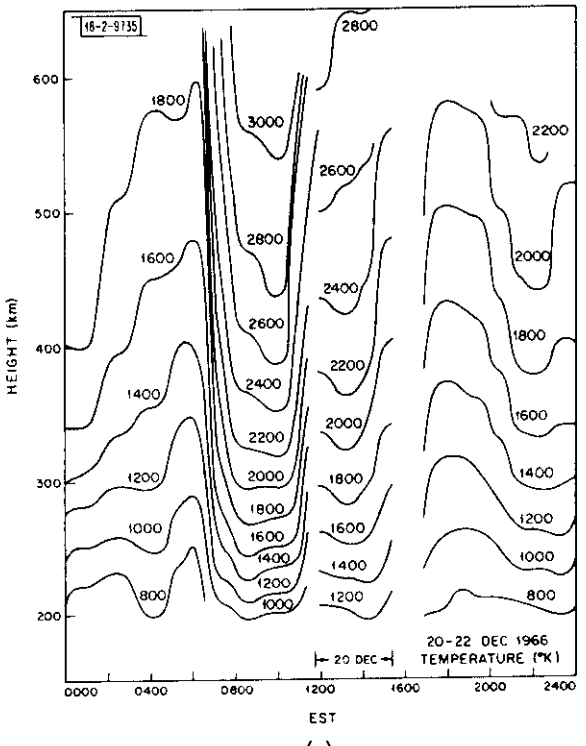

(u)

Fig. 4(a-u). Continued.

The diurnal variation of electron temperature has been discussed extensively in previous reports. The most common form of behavior is a very rapid rise in temperature during sunrise, followed by more or less steady temperatures during the daytime and a somewhat less rapid fall at sunset. Thereafter, the temperatures tend to change little during the night. This behavior can be modified in a number of recognizable ways. In winter (e.g., 14-15 January, 5-6 December), there is a period following sunset and usually lasting until midnight when the temperature rises again. We have previously attributed this to heat conducted into the ionosphere from the protonosphere which is continuously warmed by photoelectrons that escape from the conjugate hemisphere which remains sunlit. There follows a period of cooling usually beginning near midnight which is almost certainly caused by the nocturnal increase in the local density (see Sec. III).

On a number of days (e.g., 20-21 October, 20-21 December), the electron temperature reached its peak value immediately following sunrise and then decreased somewhat. This is especially noticeable at altitudes above 300 to 400 km, but this pre-noon maximum does not appear to be a regular occurrence.

A third variant of the normal behavior is observable on the days (20-21 January, 1-2 April, 22-23 August and 26-27 September) that were recognized earlier as following a storm pattern first observed in June 1965. On those days, a pronounced increase in electron density occurred somewhat before ground sunset. As a result of this, the electron temperature began to decrease much sooner than usual [see, for example, Fig. 4(m)]; no well-defined decrease occurred at sunset as is normally the case. The next morning, following sunrise, the electron density was depressed below its normal value with the result that the electron temperature rose to unusually large values.

B. Average Temperature Profiles

The tendency of the temperatures to change little during the midday period and at night has encouraged us in the past to compute average daytime and nighttime temperature profiles. This has been done for 1966 with results that are shown in Figs. 5(a) through (u). In constructing these contours, an average was taken of the temperatures observed at each 100-km height interval on all the temperature profiles available between 1000 to 1500 EST (daytime) and 2100 to 0300 EST (nighttime). These average values were then extrapolated smoothly down to a fixed value of 355°K at 120 km incorporated in the 1965 CIRA model atmospheres.

The average temperature profiles all show a monotonic increase in electron temperature with altitude. The appearance of a temperature minimum during the daytime or above $h_{max}F2$ has been reported at Jicamarca, Arecibo and St. Santin de Maurs. At Millstone, a temperature minimum was observed once in 1966 and not at all in any of the years previous when the radar was in operation (Table I). From results obtained since 1966 (unpublished), it appears that this phenomenon requires that N_{max} approach about 10^6 el/cm^3/sec, i.e., $f_oF2 \approx 10$ MHz. As can be seen in Figs. 3(a-u), the critical frequency did not begin to reach this value until toward the end of the year. A period when a temperature minimum existed for part of the afternoon is seen in Fig. 4(t) (5-6 December) when $f_oF2 > 9.5$ MHz. When these afternoon results are combined with the results for the following morning, an average daytime profile is obtained in which the minimum is obscured, and the daytime curve in Fig. 5(t) merely exhibits a kink near 300 km.

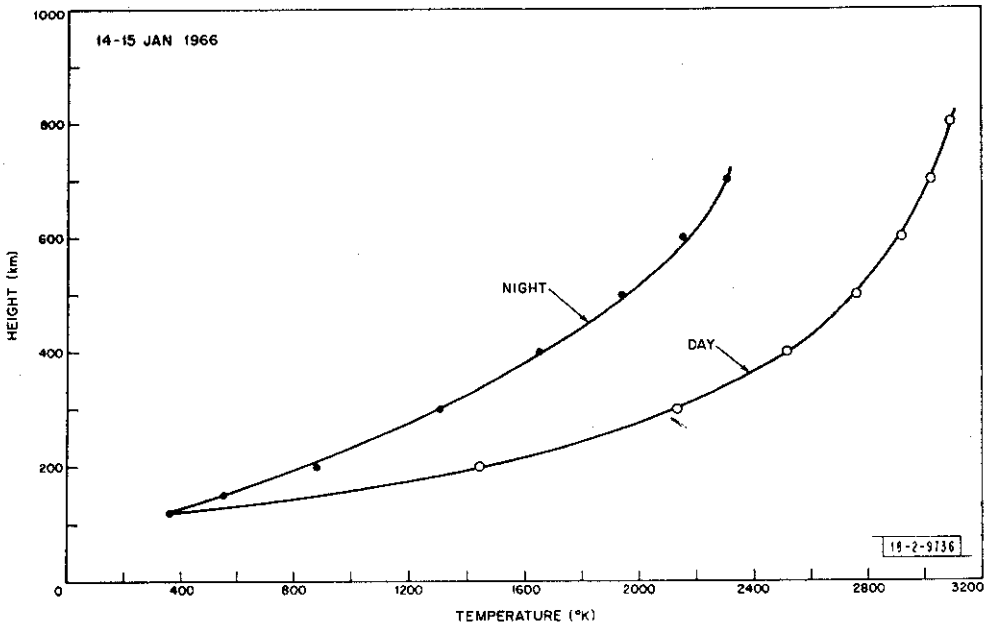

(a)

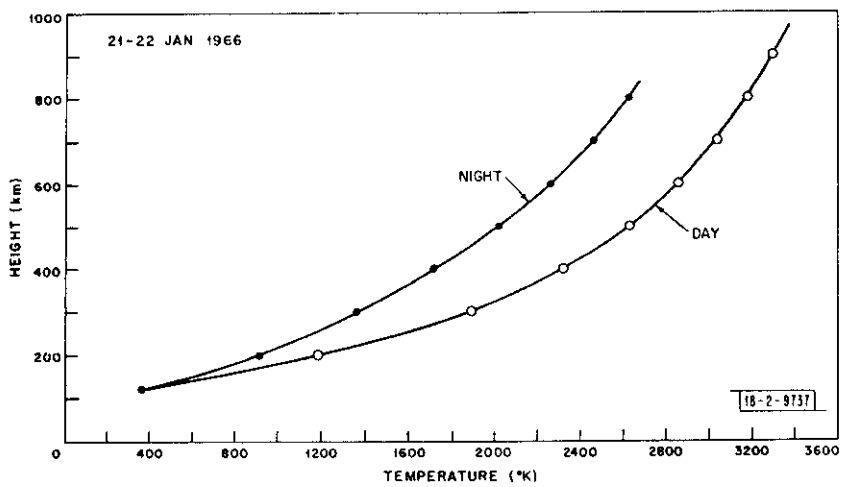

(b)

Fig. 5(a-u). Average daytime (1000 to 1500 EST) and nighttime (2100 to 0300 EST) electron temperature profiles constructed by averaging temperatures obtained in these intervals at each 100-km altitude.

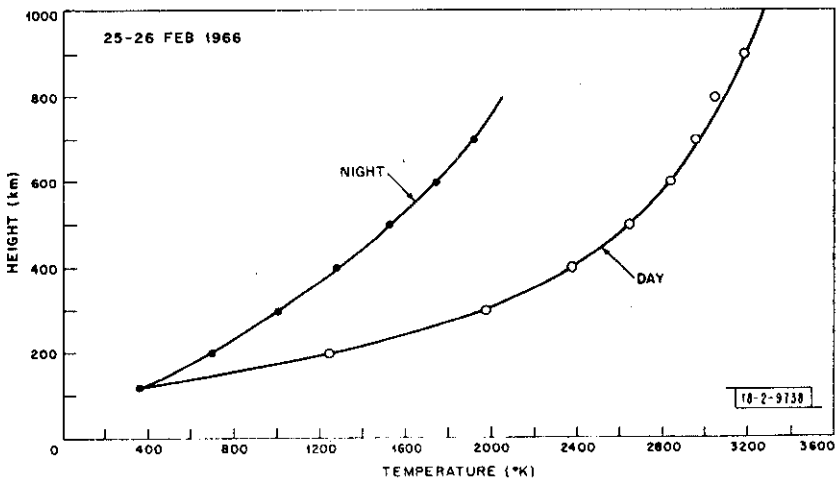

(c)

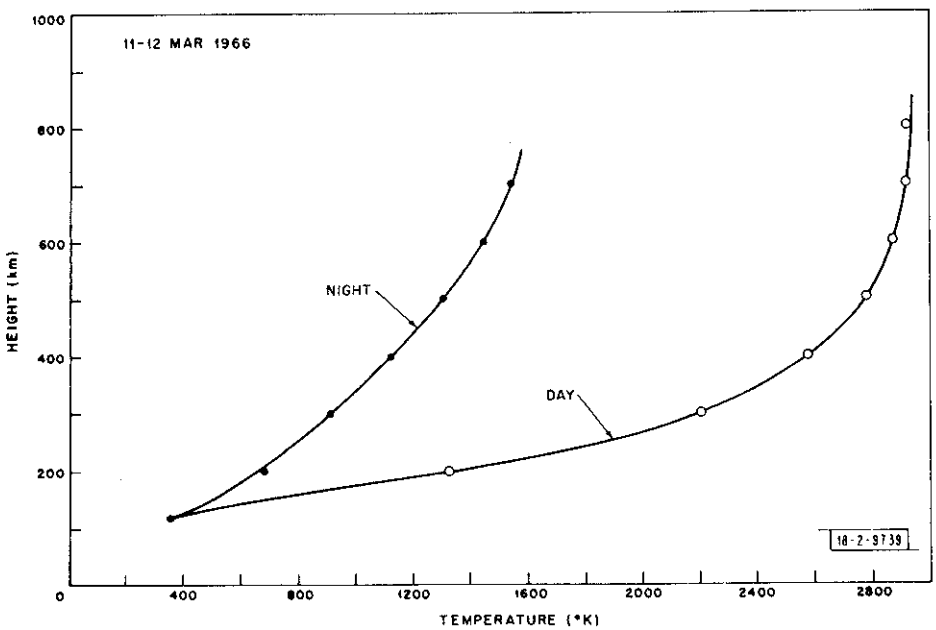

(d)

Fig. 5(a-u). Continued.

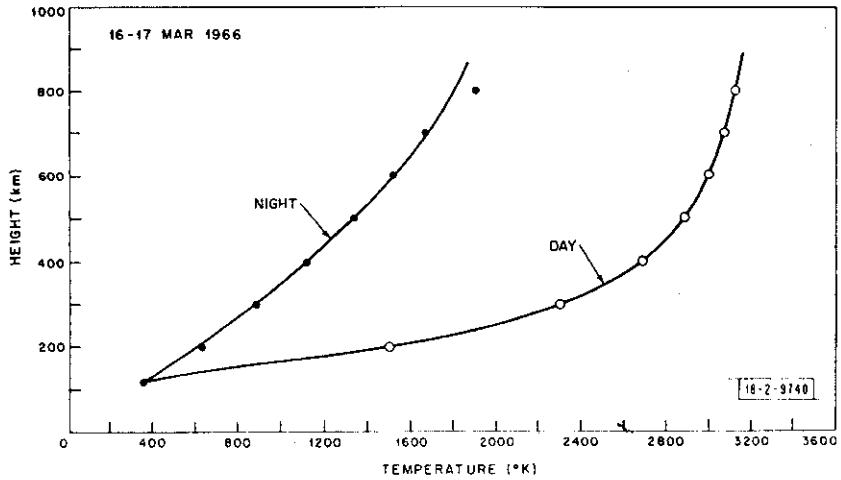

(e)

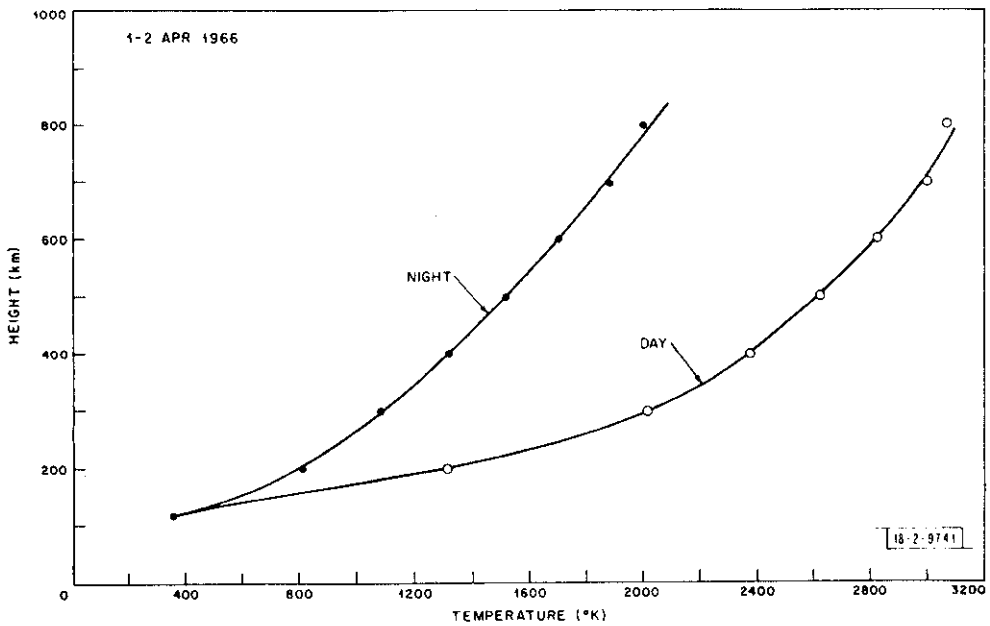

(f)

Fig. 5(a-u). Continued.

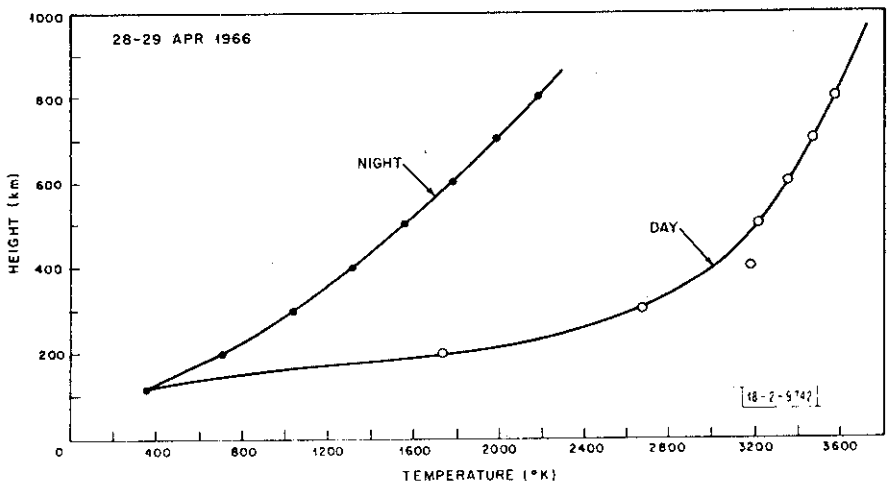

(g)

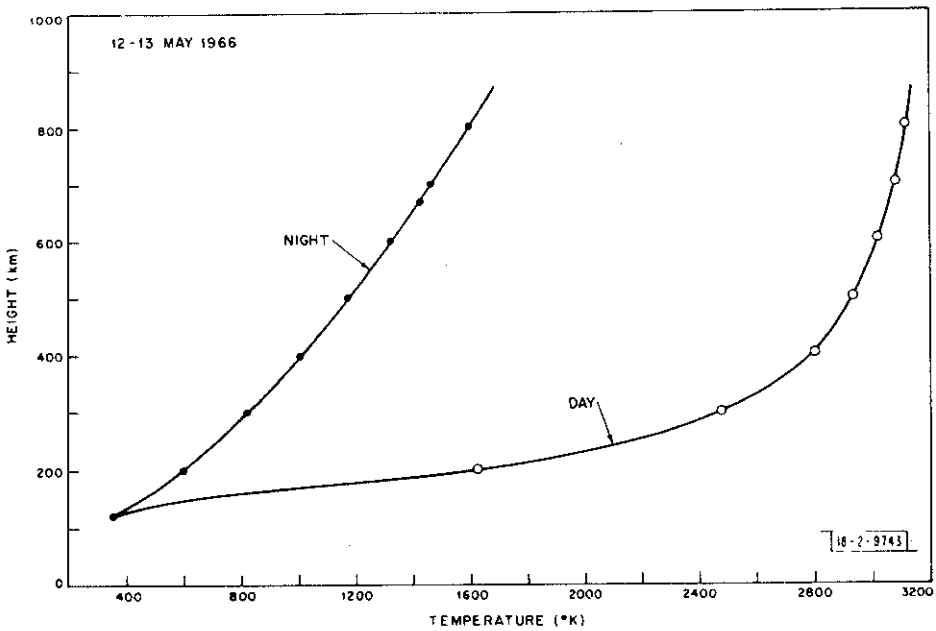

(h)

Fig. 5(a-u). Continued.

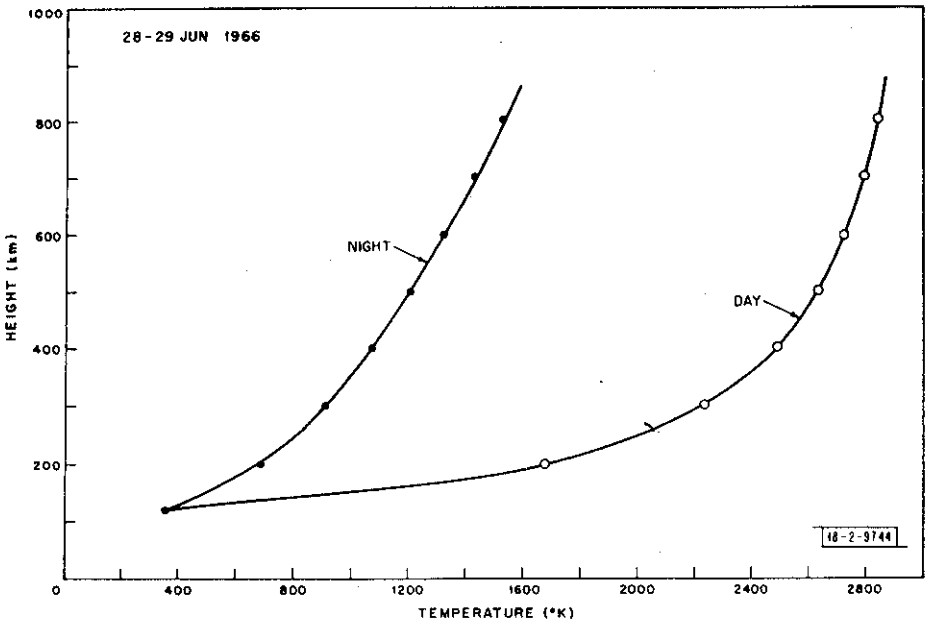

(i)

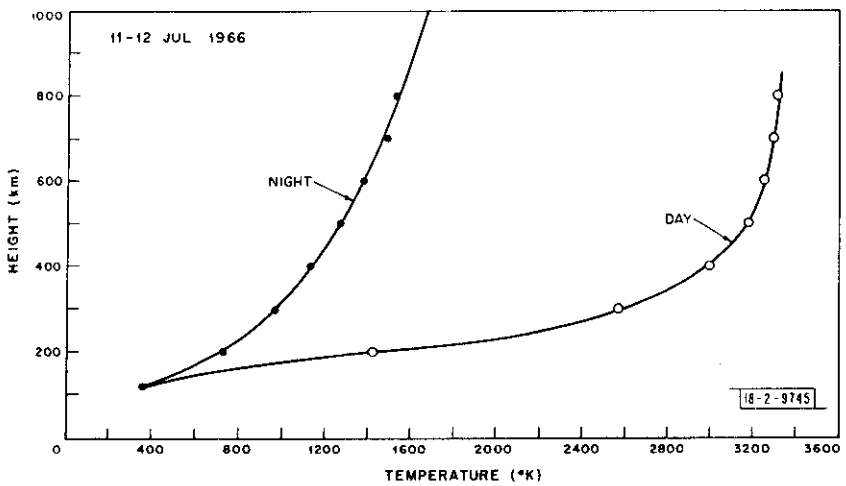

(j)

Fig. 5(a-u). Continued.

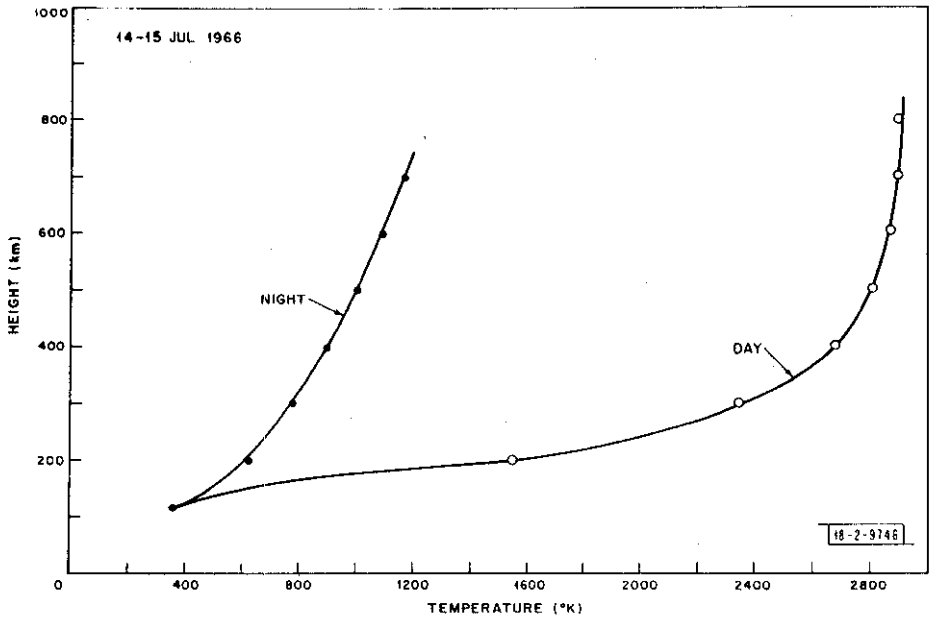

(k)

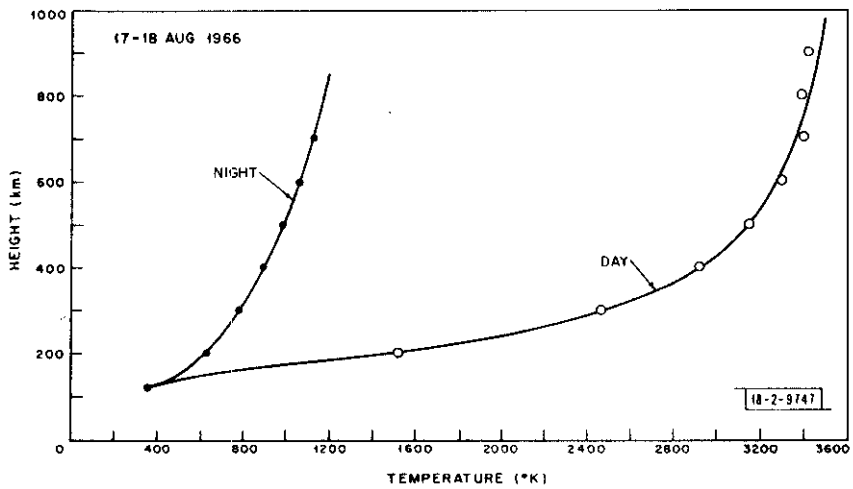

(l)

Fig. 5(a-u). Continued.

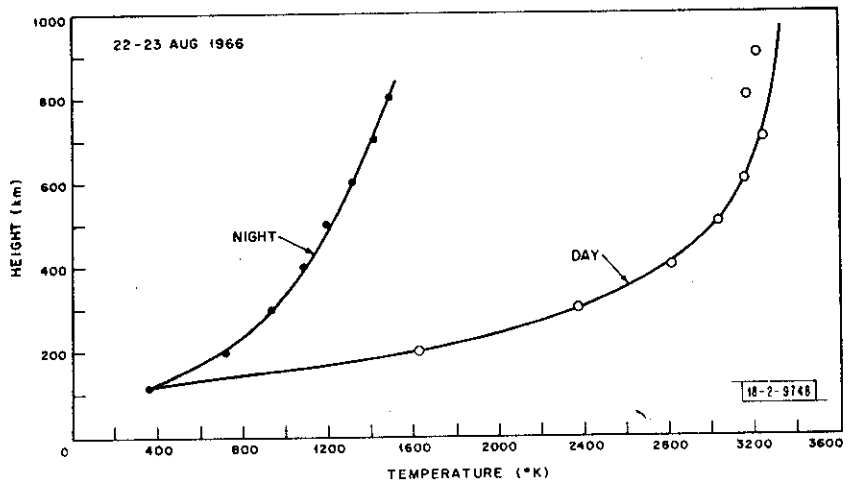

(m)

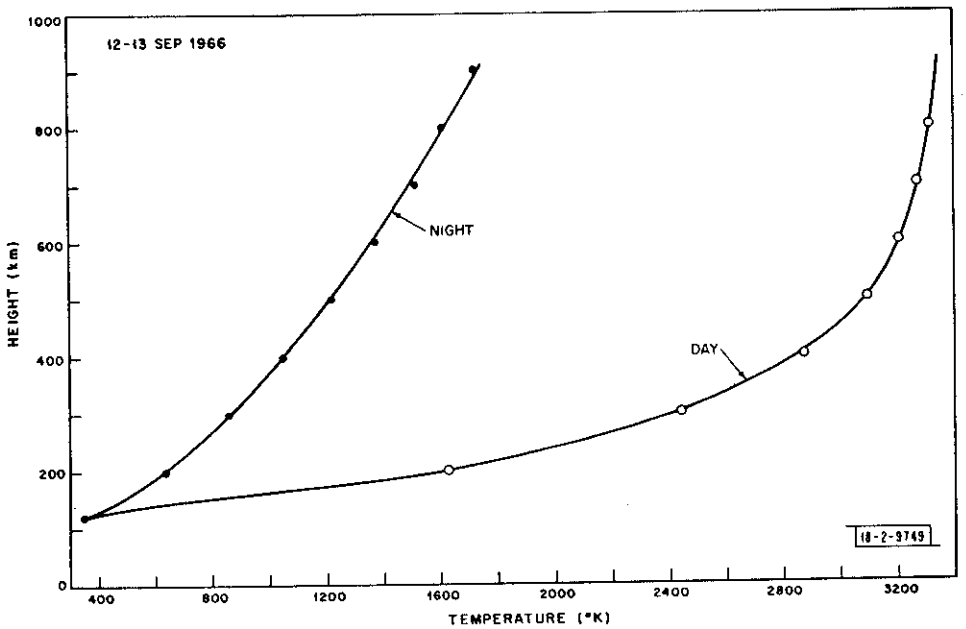

(n)

Fig. 5(a-u). Continued.

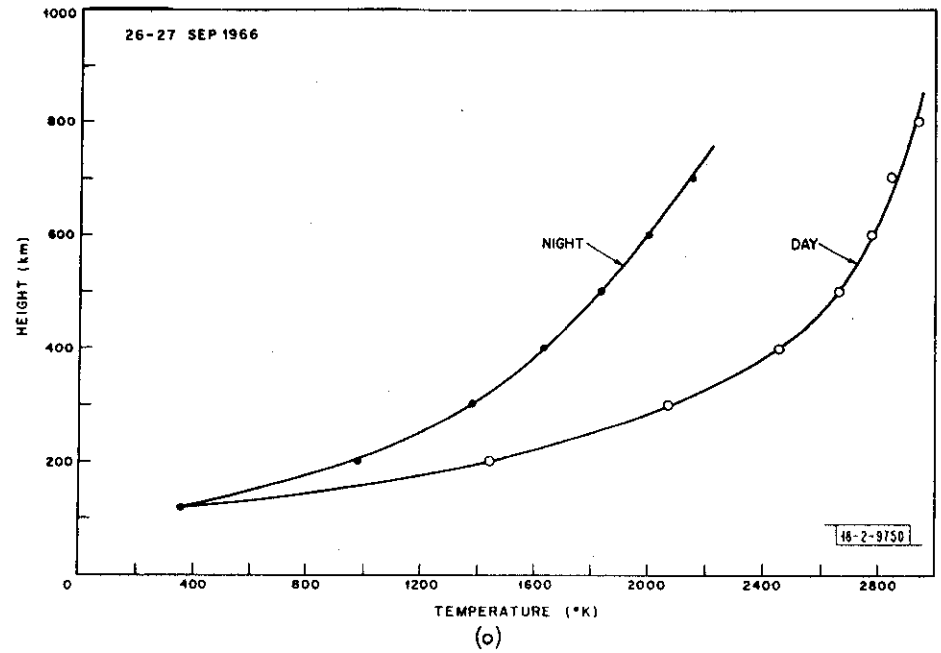

(o)

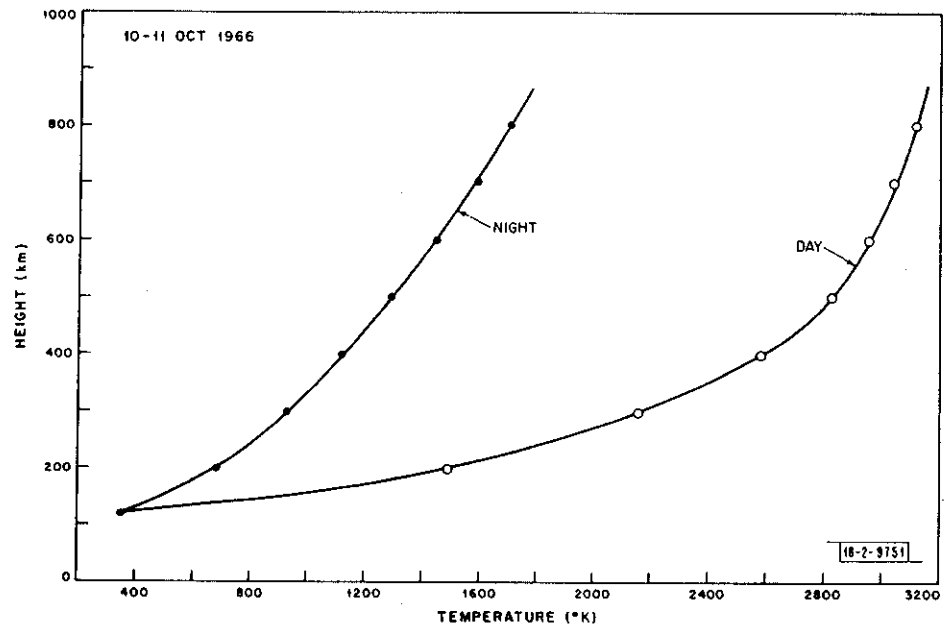

(p)

Fig. 5(a-u). Continued.

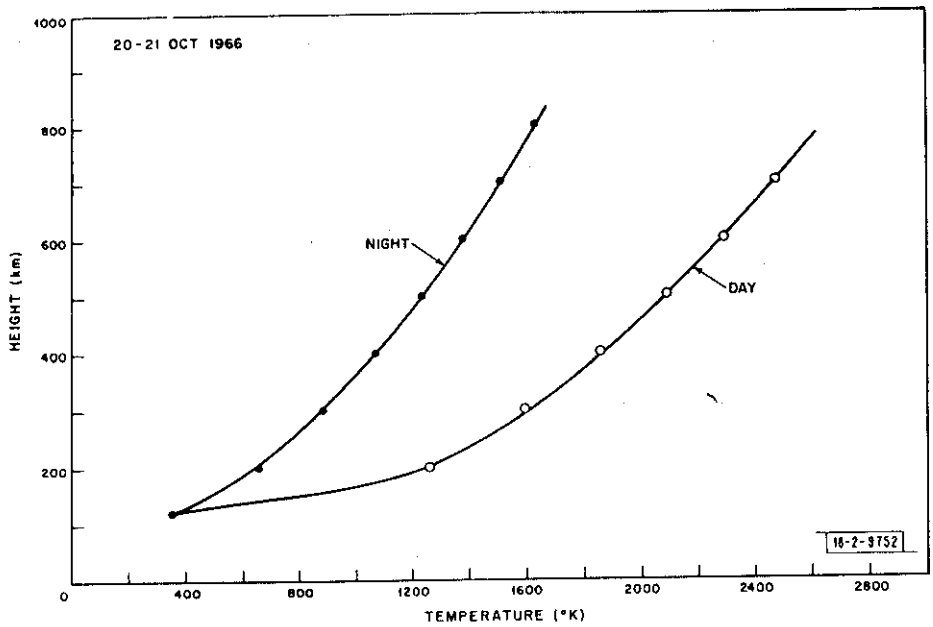

(q)

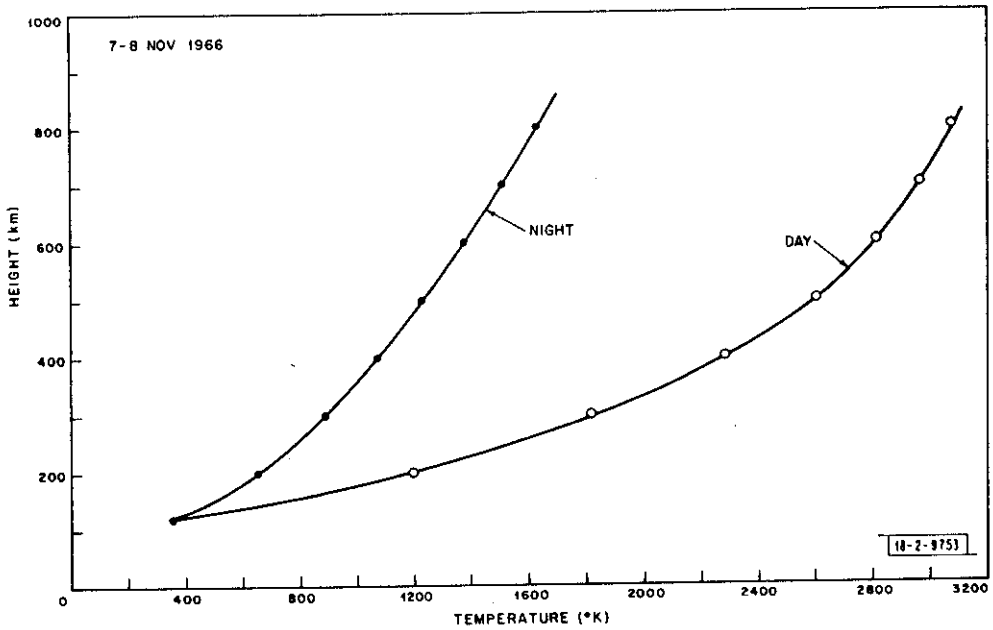

(r)

Fig. 5(a-u). Continued.

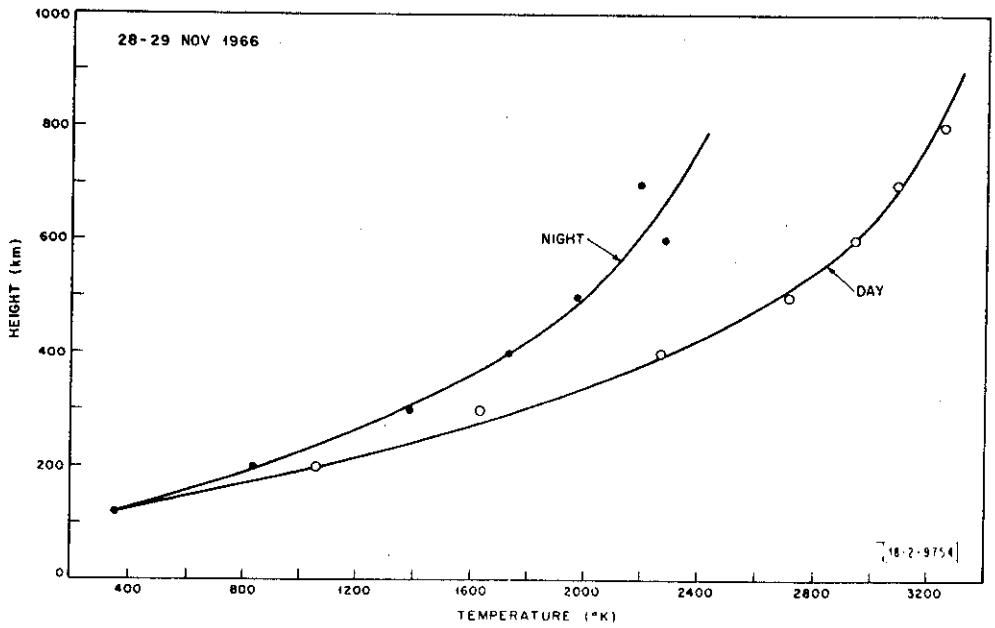

(s)

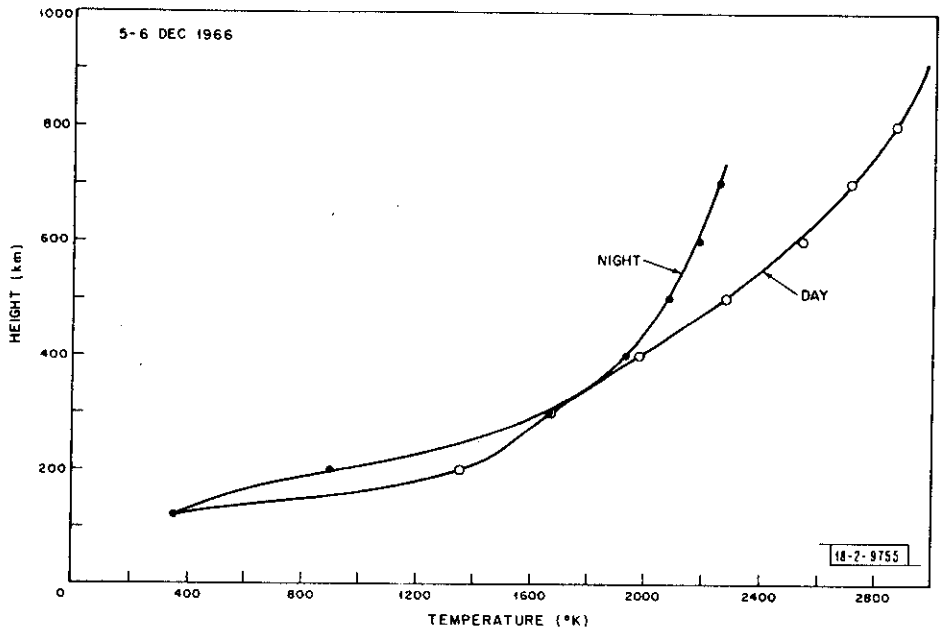

(t)

Fig. 5(a-u). Continued.

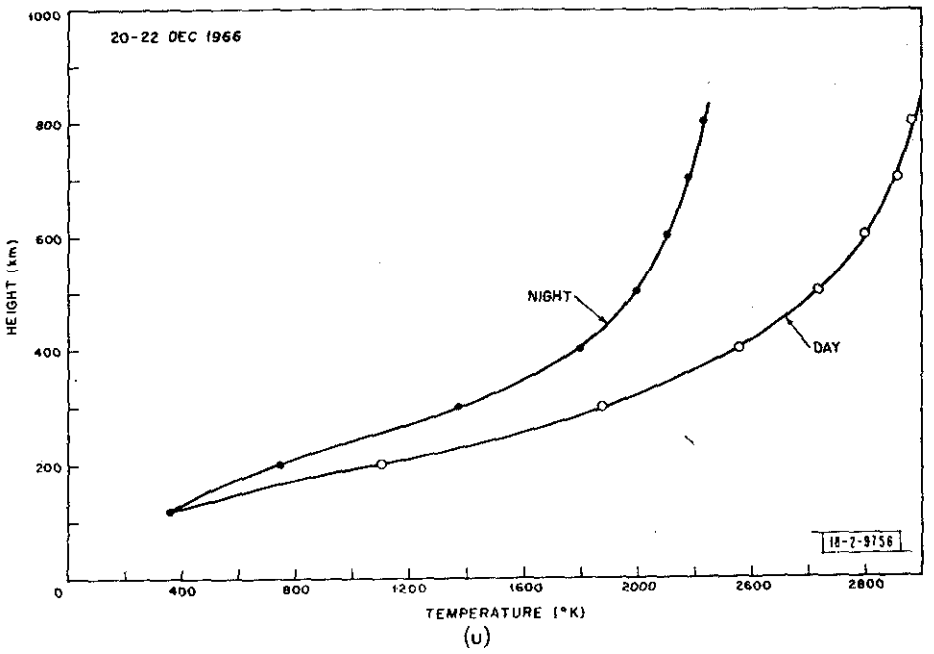

Fig. 5(a-u). Continued.

V. SEASONAL VARIATIONS

A. Electron Temperature

The average temperature plots shown in Figs. 5(a-u) have been employed to investigate seasonal variations of electron temperature. The results are shown in Figs. 6(a) and (b) and 7(a) and (b). Figure 6(a) presents a contour diagram of average electron temperature for the daytime vs height and date, and Fig. 6(b) provides a similar plot for the nighttime period. In both plots, the contour intervals are 500°K apart. The most striking feature of these plots is the higher temperatures at night in winter than in summer; this is evidence for nocturnal heat supplied from the protonosphere. Figure 7(a) shows the electron temperature at 500 and 300 km vs date for the daytime and Fig. 7(b) for the nighttime. Besides confirming the marked seasonal variation at night, these plots show the existence of a smaller but well-defined daytime variation, with the highest values being encountered in summer. Figure 7(a) supports the variations deduced for earlier years which are discussed in Ref. 10. At an altitude of 300 km, the amplitude of the variation appears to be of the order of 300° to 500°K, but probably increases with the sunspot cycle since in previous years it was not so pronounced as observed here.

The minimum in the temperature is not found in December or January as might be expected on the basis of the variation of the sun's zenith distance, but rather in October or November (see Fig. 9 of Ref. 10). It is noteworthy that $N_{max}F2$ reaches its seasonal peak at the same time and the layer thickness becomes a minimum around October-November.[6] Thus, it would seem that the seasonal variation of electron temperature is a result of the seasonal variation of F-region electron density, and is not brought about by a change in the energy flux from the sun.

Some of the structure in Figs. 6(a-b) and 7(a-b) appears to be real and associated with the magnetic storms occurring on several days as reported above. The clearest case of this association is the abnormally high temperatures encountered at night on 26-27 September [Fig. 7(b)].

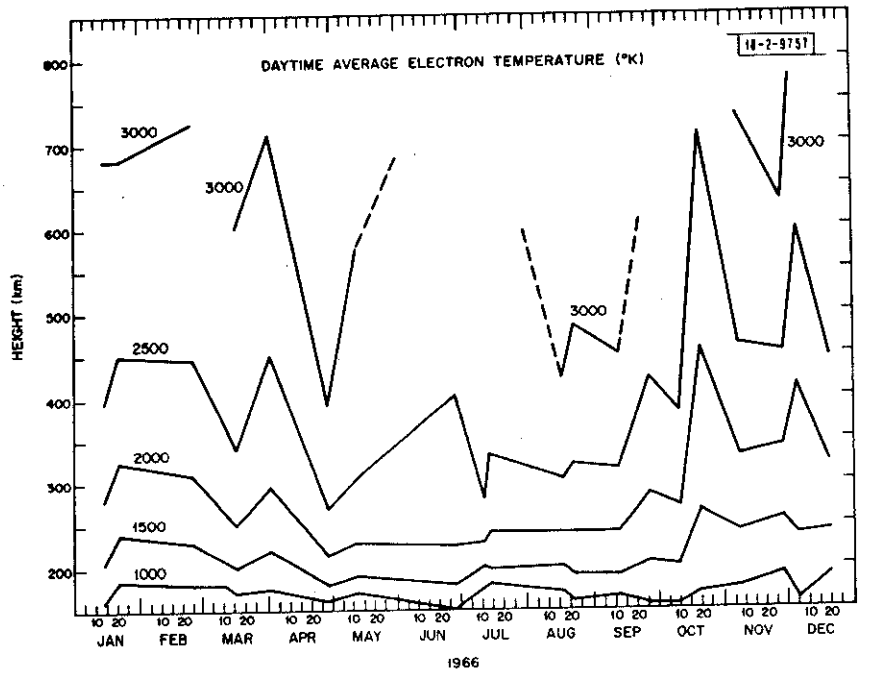

(a) Daytime (1000 to 1500 EST).

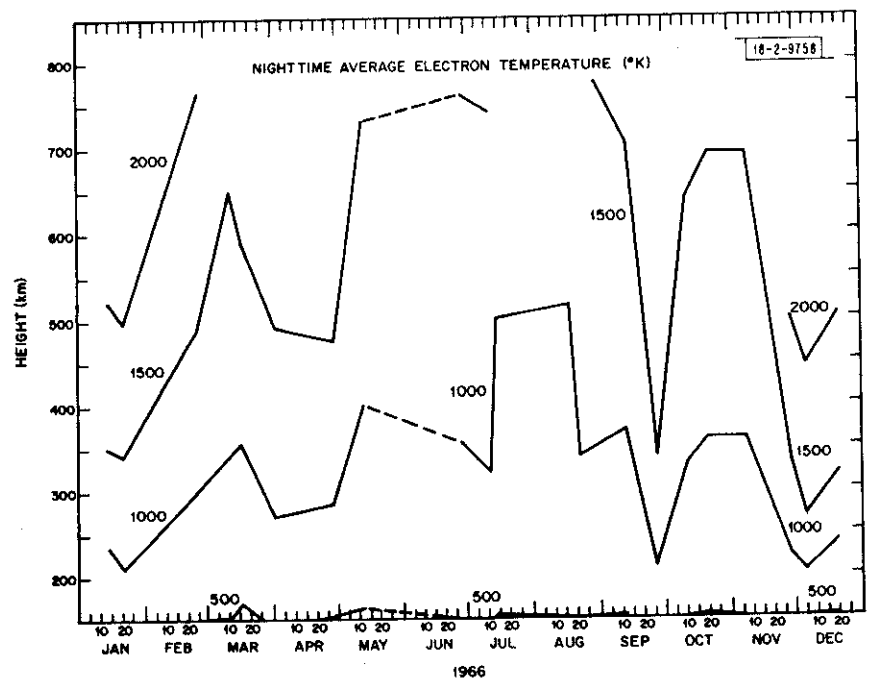

(b) Nighttime (2100 to 0300 EST).

Fig. 6(a-b). Contour plots with 500°K intervals of electron temperature vs height and season derived from average temperature profiles of Figs. 5(a-u).

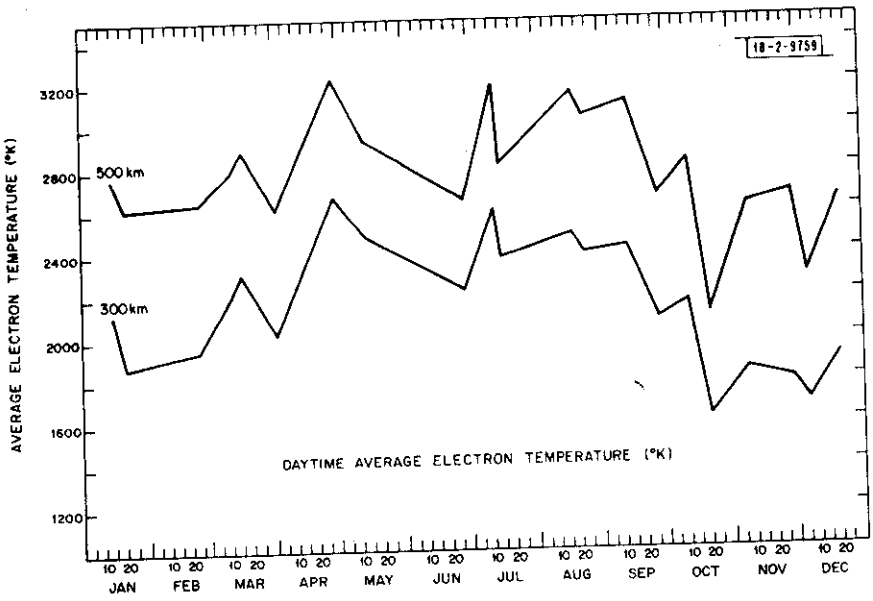

(a) Daytime (1000 to 1500 EST).

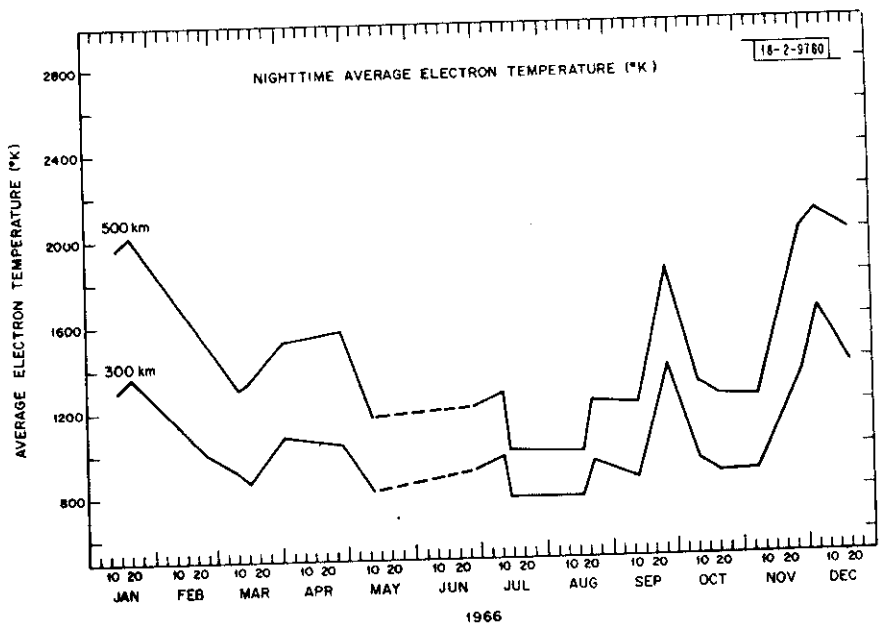

(b) Nighttime (2100 to 0300 EST).

Fig. 7(a-b). Seasonal variation of electron temperature at 300- and 500-km altitude obtained from average temperature profiles of Figs. 5(a-u).

Above-normal temperatures were also encountered on the nights of 21-22 January, 1-2 April and 22-23 August. In Refs. 7 and 8, we discussed the phenomenon of nocturnal heating related to geomagnetic storms, and showed that it is not seen at Millstone in all storms. The occurrence appears to be limited to the period of the main phase of the storm, and is accompanied by decreases in the total magnetic field observed locally. Thus, we have argued that the phenomenon is caused by heat introduced into the magnetosphere via the injection of ring current particles, and that this heat is subsequently conducted into the ionosphere. This idea was first proposed by Cole[33] to explain the stable red arc seen at midlatitudes during some geomagnetic storms, and has received support from satellite observations of the existence of high electron temperatures in such arcs.[34,35]

By contrast, the average daytime electron temperatures on the first day of a magnetic storm sometimes appear to be lower than normal,[10] due to the large electron density encountered in the late afternoon. This type of behavior has contributed to the low average temperatures observed in Fig. 7(a) on 21-22 January, 1-2 April and 26-27 September. The daytime effects are less pronounced in the average temperatures because, in several cases, abnormally low temperatures for the afternoon period have been combined with abnormally high ones encountered the next morning (when the F-layer density was low).

B. Protonospheric Heat Flux

The reason for the monotonic increase in electron temperature with altitude seen in Figs. 5(a-u) lies in the existence of a flux of heat conducted along the magnetic field lines from the protonosphere into the ionosphere. We have shown elsewhere[36-38] that the most likely source of this heating, under normal conditions, is the escape of photoelectrons from the ionosphere and the subsequent deposition of a large fraction of the photoelectron energy in the magnetosphere via encounters with ambient electrons. As such, the observed heat flux should place a lower limit on the total escaping energy in the photoelectron flux. From the observations made in 1964, we deduced that the energy in the escape flux must exceed 5×10^9 eV/cm^2/sec.[36,37] This is in accord with calculations of the escape energy performed by Fontheim, et al.,[39] Duboin, et al.,[40] Nisbet,[41] and Nagy, et al.,[42] among others. Experimental estimates of the escape flux have been made from temperature profile measurements by Sanatani and Hanson,[43] Bauer, et al.,[44] and from direct satellite observations by Rao and Maier,[45,46] which are as large or larger than our estimate.

Despite this large amount of effort, there remains some uncertainty in the fraction of the energy extracted from the photoelectron flux in the magnetosphere. In part, this arises because early workers neglected the backscattering of photoelectrons arriving at the conjugate ionosphere. Experimentally, this has been observed through plasma-line observations at Millstone[47] and in direct satellite measurements.[45] This phenomenon may cause as much as 50 percent of the flux of particles arriving at the conjugate hemisphere to be scattered back along the field line, and thus tends to increase the energy deposited in the magnetosphere.[48] Only in one recent paper (Nagy and Banks[49]) has it been fully included. In most papers, the rate of loss of photoelectron energy per unit path length in the magnetosphere has been taken as[50]

$$\frac{dE}{ds} = -1.95 \times 10^{-12} \frac{N}{E} \text{ eV/cm} \qquad (1)$$

where E is the photoelectron energy, s is the path length, and N is the density of the ambient electrons. It has recently been suggested that this equation underestimates the loss rate for

photoelectrons.[51] Thus, at high latitudes, it may be that almost all the energy in the escaping flux is deposited in the magnetosphere.

We have attempted to calculate the heat flux Q entering the ionosphere from the magnetosphere along the lines of force from the observed electron temperature gradient dT_e/dh and temperature T_e through

$$Q = 7.7 \times 10^5 T_e^{5/2} \frac{dT_e}{dh} \sin^2 I \text{ eV/cm}^2 \quad (2)$$

where I is the dip angle of the earth's magnetic field. In order to employ Eq. (2) to estimate the arriving heat flux, it is necessary to make measurements at an altitude substantially above the height where the rate of local heat loss from the electrons to the ions has become important.[38,44] Accordingly, dT_e/dh was estimated from the temperature differences observed over each 100-km interval above 500 km for the mean temperature profiles shown in Figs. 5(a-u). The heat flux was then calculated via Eq. (2) employing the mean value of T_e for that interval, and an average of the separate estimates of Q was then taken. The values of Q obtained in this way from the mean daytime and nighttime temperature profiles are shown in Figs. 8(a) and (b). Figure 8(a) shows that in 1966 the average daytime heat flux was about 4×10^9 eV/cm^2/sec, i.e., somewhat larger than the value of 2 to 3×10^9 eV/cm^2/sec observed in 1965 (Ref. 10). Results obtained during 1964 appeared to show a seasonal variation of the daytime flux with a minimum in local summer. The results for 1965 (Ref. 10) and those presented here [Fig. 8(a)] seem to support this but do not exhibit as large a variation (2:1) as found in 1964. The exact source of a seasonal variation, if real, is not clear at present.

The nighttime flux [Fig. 8(b)] shows a marked seasonal variation expected as a consequence of the sun being above the horizon at the conjugate point at night in local winter. In local summer, the flux falls to an extremely small value set by the cooling of the protonosphere.

Some peaks in Figs. 8(a-b) appear to be real and associated with the magnetic disturbances. Thus, we believe that the high values seen in Fig. 8(a) on 22 January, 23 August and 29 November

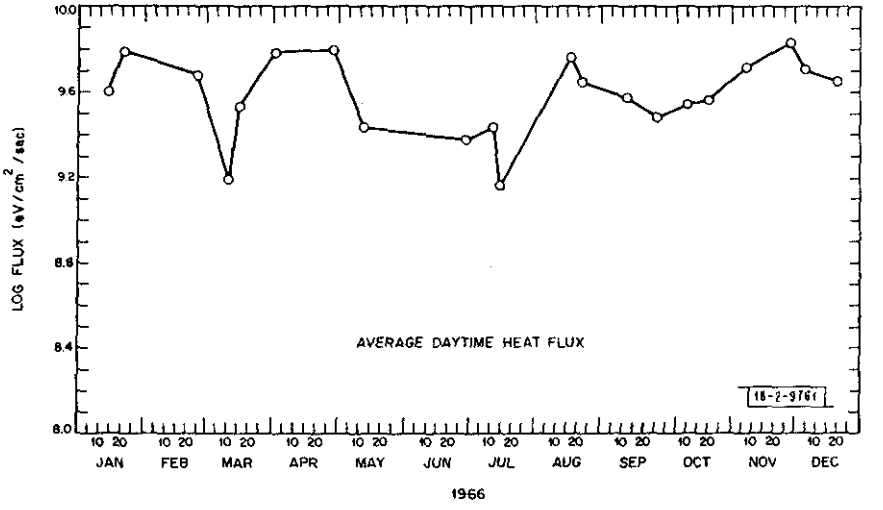

(a) Daytime (1000 to 1500 EST).

Fig. 8(a-b). Heat flux carried into ionosphere via electron gas as deduced from average temperature profiles of Figs. 5(a-u) vs season.

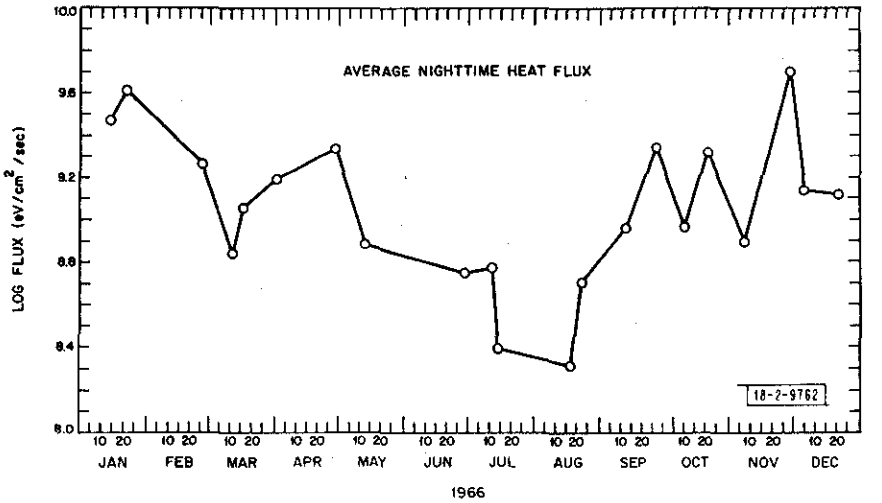

(b) Nighttime (2100 to 0300 EST).

Fig. 8(a-b). Continued.

are manifestations of additional heat being supplied to the ionosphere from the protonosphere on those days. Similarly, the peaks in Fig. 8(b) on the nights of 21-22 January, 26-27 September and 28-29 November probably represent nocturnal heating events associated with storms. As discussed above, this heating appears to coincide with the main phase of the storm and probably is caused by heat deposition in the magnetosphere through the loss of energy of ring current protons (possibly through ion-cyclotron damping by ambient electrons).

VI. SUMMARY

The Millstone Hill Thomson scatter radar was employed to measure F-region electron densities and temperatures during 1966 for periods of 24 hours at a time, approximately twice per month. The measurements yielded an electron density and temperature profile over the height interval roughly 150 to 750 km in a time interval of 30 minutes. These data have been used to construct contour diagrams showing the variation of density and temperature as a function of height and time for each of the periods of observation [Figs. 3(a-u) and 4(a-u)]. These plots show greater structure than found heretofore, partly as a result of the improved time resolution of the measurements and the fact that mean monthly averages have not been presented. We also believe that there has been a real increase in the hour-to-hour variability of the ionosphere resulting from increased fluctuation of the solar EUV output and the presence of traveling ionospheric disturbances.

Despite this, the results follow trends recognized for the data collected in 1964 (Ref. 2) and 1965 (Ref. 3). A number of days appear to have been magnetically disturbed, and at least four (21-22 January, 1-2 April, 22-23 August and 26-27 September) exhibit a characteristic storm behavior first witnessed in June 1965 (Ref. 9). Late in the afternoon of the first storm day, the layer was lifted to an abnormal height and simultaneously achieved higher-than-normal densities. The great height of the layer and large density appear to have been responsible for lower-than-normal electron temperature. We attribute this behavior to an east-west electric field that propagates into the ionosphere along magnetic field lines from the magnetosphere. The electric field

is produced by charge separation of the plasma injected into the evening sector and responsible for the asymmetric portion of the ring current. The electric field produces an E × B drift directed north and upward, and hence opposes the downward diffusion of ionization due to gravity and neutral winds.

On the following morning, the reverse behavior is often encountered – the peak density is low and the electron temperature is high. We believe this is caused by composition changes (principally a large increase in N_2) brought about by the heating of the auroral regions.[15,31]

The results have also been employed to construct average daytime and nighttime temperature profiles from which seasonal variations in the temperature and heat flux conducted into the ionosphere can be examined. We find a significant increase (300° to 400°K) in the summer daytime temperatures over the winter ones that is probably caused by the seasonal variation of electron density. The average heat flux conducted into the ionosphere from the protonosphere in the daytime shows a slight seasonal variation of the opposite kind (winter > summer), but no explanation for this has been offered. A large nighttime variation is evident (winter temperatures exceeding summer ones) and is believed to be caused by the heating of the protonosphere by photoelectrons escaping from the conjugate point which remains sunlit in winter.

ACKNOWLEDGMENTS

The author would like to acknowledge the efforts of W. Abel, W.A. Reid and J.H. McNally in collecting these data; also, R. Julian, J.K. Upham, Mrs. A. Freeman, Miss D. Tourigny and Miss L. Zak in various portions of the data reduction. The continued support of P.B. Sebring is also gratefully acknowledged.

REFERENCES

1. J.V. Evans, "Ionospheric Backscatter Observations at Millstone Hill," Technical Report 374, Lincoln Laboratory, M.I.T. (22 January 1965), DDC AD-616607.
2. _____, "Millstone Hill Thomson Scatter Results for 1964," Technical Report 430, Lincoln Laboratory, M.I.T. (15 November 1967), DDC AD-668436.
3. _____, "Millstone Hill Thomson Scatter Results for 1965," Technical Report 474, Lincoln Laboratory, M.I.T. (8 December 1969), DDC AD-707501.
4. _____, *Planet. Space Sci.* 13, *1031 (1965), DDC AD-616607.*
5. _____, J. Geophys. Res. 70, 1175 (1965), DDC AD-614310.
6. _____, Planet. Space Sci. 15, 1387 (1967).
7. _____, J. Geophys. Res. 75, 4803 (1970), DDC AD-714447.
8. _____, J. Geophys. Res. 75, 4815 (1970), DDC AD-714446.
9. _____, J. Atmos. Terr. Phys. 32, 1629 (1970), DDC AD-716057.
10. _____, Planet. Space Sci. 18, 1225 (1970), DDC AD-716056.
11. _____, R.F. Julian and W.A. Reid, "Incoherent Scatter Measurements of F-Region Density, Temperatures, and Vertical Velocity at Millstone Hill," Technical Report 477, Lincoln Laboratory, M.I.T. (6 February 1970), DDC AD-706863.
12. G.A.M. King, Planet. Space Sci. 9, 95 (1962).
13. _____, J. Atmos. Terr. Phys. 30, 1733 (1968).
14. R.A. Duncan, Planet. Space Sci. 17, 841 (1969).
15. R.B. Norton, Proc. IEEE 57, 1147 (1969).
16. G. Thome, J. Geophys. Res. 73, 6319 (1968).
17. J. Testud and G. Vasseur, Ann. Geophys. 25, 525 (1969).
18. M.J. Davis and A.V. daRosa, J. Geophys. Res. 74, 5721 (1969).
19. *W. Blumen and R. Hendl*, J. *Atmos. Sci.* 26, 210 (1969).
20. G. Chimonas and C.O. Hines, Planet. Space Sci. 18, 565 (1970).
21. J.V. Evans, J. Geophys. Res. 70, 4331 (1965), DDC AD-623606.
22. H. Rishbeth, J. Atmos. Terr. Phys. 30, 63 (1968).
23. G. Vasseur, J. Atmos. Terr. Phys. 32, 775 (1970).
24. J.A. Klobuchar, J. Aarons and H. Hejeb Hosseinieh, J. Geophys. Res. 73, 7530 (1968).
25. J.A. Ratcliffe, J. Geophys. Res. 56, 463 (1951).
26. B. Chatterjee, J. Geophys. Res. 58, 353 (1953).
27. H. Kohl, J.W. King and D. Eccles, J. Atmos. Terr. Phys. 30, 1733 (1968).
28. H. Rishbeth and C.S.G.K. Setty, J. Atmos. Terr. Phys. 20, 263 (1961).
29. J.V. Evans, J. Geophys. Res. 72, 3343 (1967), DDC AD-658912.
30. _____ *and L.P. Cox, J. Geophys. Res.* 75, 159 (1970), DDC AD-703492.
31. L.P. Cox and J.V. Evans, J. Geophys. Res. 75, 6271 (1970).
32. M. Mendillo, M.D. Papagiannis and J.A. Klobuchar, Radio Sci. 5, 895 (1970).
33. K.D. Cole, J. Geophys. Res. 70, 1689 (1965).
34. R.B. Norton and J.A. Findlay, Planet. Space Sci. 17, 1867 (1969).
35. J.A. Findlay, P.L. Dyson, L.H. Brace, A.J. Zmuda and W.E. Radford, J. Geophys. Res. 74, 3705 (1969).
36. J.V. Evans, Planet. Space Sci. 15, 1557 (1967).
37. _____, Space Research VIII (North Holland Publishing Co., Amsterdam, 1968), p. 717.
38. _____ and G.P. Mantas, J. Atmos. Terr. Phys. 30, 563 (1968).

39. E.G. Fontheim, A.E. Beutler and A.F. Nagy, Ann. Géophys. 24, 489 (1968).

40. M.L. Duboin, G. Lejeune, M. Petit and G. Weill, J. Atmos. Terr. Phys. 30, 299 (1968).

41. J.S. Nisbet, J. Atmos. Terr. Phys. 30, 1257 (1968).

42. A.F. Nagy, E.G. Fontheim, R.S. Stolarski and A.E. Beutler, J. Geophys. Res. 74, 4667 (1969).

43. S. Sanatani and W.B. Hanson, J. Geophys. Res. 75, 469 (1970).

44. P. Bauer, G. Lejeune and M. Petit, Planet. Space Sci. 18, 1447 (1970).

45. B.C.N. Rao and E.J.R. Maier, J. Geophys. Res. 75, 816 (1970).

46. E.J.R. Maier and B.C.N. Rao, J. Geophys. Res. 75, 7168 (1970).

47. J.V. Evans and I.J. Gastman, J. Geophys. Res. 75, 807 (1970), DDC AD-704626.

48. P.M. Banks and A.F. Nagy, J. Geophys. Res. 75, 1902 (1970).

49. A.F. Nagy and P.M. Banks, paper presented at the XIII Planetary Meeting of COSPAR, Leningrad, 20-29 May 1970.

50. A. Dalgarno, M.B. McElroy and R.J. Moffett, Planet. Space Sci. 11, 463 (1963).

51. A.F. Nagy, private communication (1970).

DOCUMENT CONTROL DATA – R&D

(Security classification of title, body of abstract and indexing annotation must be entered when the overall report is classified)

1. ORIGINATING ACTIVITY *(Corporate author)* Lincoln Laboratory, M.I.T.	2a. REPORT SECURITY CLASSIFICATION Unclassified 2b. GROUP None

3. REPORT TITLE

Millstone Hill Thomson Scatter Results for 1966

4. DESCRIPTIVE NOTES *(Type of report and inclusive dates)*
Technical Report

5. AUTHOR(S) *(Last name, first name, initial)*

Evans, John V.

6. REPORT DATE 19 January 1971	7a. TOTAL NO. OF PAGES 48	7b. NO. OF REFS 51
8a. CONTRACT OR GRANT NO. F19628-70-C-0230 b. PROJECT NO. 7X263304D215 c. d.	9a. ORIGINATOR'S REPORT NUMBER(S) Technical Report 481 9b. OTHER REPORT NO(S) *(Any other numbers that may be assigned this report)* ESD-TR-71-7	

10. AVAILABILITY/LIMITATION NOTICES

Approved for public release; distribution unlimited.

11. SUPPLEMENTARY NOTES None	12. SPONSORING MILITARY ACTIVITY Office of the Chief of Research and Development, Department of the Army

13. ABSTRACT

This report presents F-region electron densities and electron temperatures observed during the year 1966 at the Millstone Hill Radar Observatory (42.6°N, 71.5°W) by the UHF Thomson (incoherent) scatter radar. The measurements were usually made for periods of 24 hours twice per month, and covered the altitude range 150 to 750 km approximately. The time required to collect all the measurements spanning this height interval was 30 minutes, i.e., half that of previous years. The results exhibit a greater amount of random time variation than seen heretofore, partly as a result of the better time resolution achieved and partly because each day has been analyzed individually, i.e., we have discontinued the practice of computing only the monthly mean behavior. We believe, however, that the largest part of the random variation is real and results from fluctuations in the solar EUV flux, which increase in magnitude as the sunspot number rises. Also, we expect a growing incidence of fluctuations produced by large-scale traveling ionospheric disturbances as we approach sunspot maximum. Despite this variability, the characteristic "winter" and "summer" type behavior reported for Millstone in previous years is clearly recognizable. On four days in which pronounced effects due to geomagnetic storms are evident, the layer rose to great heights in the late afternoon and achieved an abnormally high density (and lower-than-normal temperature). The reverse behavior was encountered the next morning. This sequence is similar to that first seen in June 1965, and its interpretation in terms of current ideas is summarized.

14. KEY WORDS

Millstone radar
F-region
diurnal variations
electron density
ionospheric scatter
seasonal variations
temperature effects
spectrum analyzers

☆ U. S. GOVERNMENT PRINTING OFFICE: 1971—433-280/24